

การพัฒนาพอลิเบนซอกซาซินเดิมกราไฟท์/กราฟีนที่นำความร้อนสูง สำหรับเป็นแผ่นไบโพลาร์ในเซลล์
เชื้อเพลิง



บทคัดย่อและแฟ้มข้อมูลฉบับเต็มของวิทยานิพนธ์ตั้งแต่ปีการศึกษา 2554 ที่ให้บริการในคลังปัญญาจุฬาฯ (CUIR)
เป็นแฟ้มข้อมูลของนิสิตเจ้าของวิทยานิพนธ์ ที่ส่งผ่านทางบัณฑิตวิทยาลัย

The abstract and full text of theses from the academic year 2011 in Chulalongkorn University Intellectual Repository (CUIR)
are the thesis authors' files submitted through the University Graduate School.

วิทยานิพนธ์นี้เป็นส่วนหนึ่งของการศึกษาตามหลักสูตรปริญญาวิศวกรรมศาสตรมหาบัณฑิต
สาขาวิชาวิศวกรรมเคมี ภาควิชาวิศวกรรมเคมี
คณะวิศวกรรมศาสตร์ จุฬาลงกรณ์มหาวิทยาลัย
ปีการศึกษา 2558
ลิขสิทธิ์ของจุฬาลงกรณ์มหาวิทยาลัย

Development of Highly Thermally Conductive Graphite/Graphene Filled Polybenzoxazine
for Bipolar Plates in Fuel Cells

Miss Manlika Phuangngamphan



A Thesis Submitted in Partial Fulfillment of the Requirements
for the Degree of Master of Engineering Program in Chemical Engineering

Department of Chemical Engineering

Faculty of Engineering

Chulalongkorn University

Academic Year 2015

Copyright of Chulalongkorn University

Thesis Title	Development of Highly Thermally Conductive Graphite/Graphene Filled Polybenzoxazine for Bipolar Plates in Fuel Cells
By	Miss Manlika Phuangngamphan
Field of Study	Chemical Engineering
Thesis Advisor	Associate Professor Sarawut Rimdusit, Ph.D.

Accepted by the Faculty of Engineering, Chulalongkorn University in Partial Fulfillment of the Requirements for the Master's Degree

.....Dean of the Faculty of Engineering
(Associate Professor Supot Teachavorasinskun, D.Eng.)

THESIS COMMITTEE

.....Chairman
(Associate Professor Siriporn Damrongsakkul, Ph.D.)

.....Thesis Advisor
(Associate Professor Sarawut Rimdusit, Ph.D.)

.....Examiner
(Paravee Vas-Umnuay, Ph.D.)

.....External Examiner
(Assistant Professor Chanchira Jubslip, D.Eng.)

มัลลิกา พ่วงงามพันธุ์ : การพัฒนาพอลิเบนซอกซาซีนเติมกราไฟท์/กราฟีนที่นำความร้อนสูงสำหรับเป็นแผ่นไบโพลาร์ในเซลล์เชื้อเพลิง (Development of Highly Thermally Conductive Graphite/Graphene Filled Polybenzoxazine for Bipolar Plates in Fuel Cells) อ.ที่ปรึกษาวิทยานิพนธ์หลัก: รศ. ดร. ศราวุธ ริมดุสิต, 112 หน้า.

งานวิจัยนี้ทำการศึกษาและพัฒนาแผ่นพอลิเมอร์คอมพอสิตไบโพลาร์ ที่มีสมบัติการนำความร้อนและนำไฟฟ้าสูง และสมบัติทางกลที่ดี เพื่อนำไปประยุกต์ใช้เป็นแผ่นไบโพลาร์ในเซลล์เชื้อเพลิงชนิดเยื่อแลกเปลี่ยนโปรตอน (PEMFC) โดยแผ่นไบโพลาร์ต้องมีค่าการนำไฟฟ้าและค่าการนำความร้อนที่สูง มีสมบัติทางกลที่ดี ดังนั้นในงานวิจัยนี้จึงมีวัตถุประสงค์เพื่อศึกษาสมบัติดังกล่าวของพอลิเมอร์คอมพอสิตจากกราไฟท์ กราฟีน และพอลิเบนซอกซาซีน งานวิจัยจะเลือกใช้กราไฟท์ขนาดใหญ่มีขนาดอนุภาคเฉลี่ย 240 ไมโครเมตร ในการทดลองจะเติมกราไฟท์และกราฟีนรวมกันในอัตราส่วนร้อยละ 83 โดยน้ำหนักลงในพอลิเบนซอกซาซีนซึ่งใช้เป็นเมทริกซ์ และศึกษาผลของการเติมกราฟีนลงไปแทนที่กราไฟท์อยู่ในช่วงร้อยละ 0 ถึง 10 โดยน้ำหนัก พบว่าค่ามอดูลัสของระบบอุณหภูมิห้องที่เติมกราฟีนร้อยละ 7.5 โดยน้ำหนัก มีค่า 16.9 จิกะปาสคาล ซึ่งมีค่าเพิ่มขึ้นถึงร้อยละ 186 เมื่อเทียบกับพอลิเบนซอกซาซีนเมทริกซ์ที่มีค่า 5.9 จิกะปาสคาล นอกจากนี้ยังพบว่าอุณหภูมิการเปลี่ยนสถานะคล้ายแก้ว (T_g) ของกราไฟท์/กราฟีนคอมพอสิตอยู่ในช่วงระหว่าง 200 ถึง 209 องศาเซลเซียส ซึ่งเพิ่มขึ้นตามปริมาณกราฟีนที่เพิ่มสูงขึ้น ทั้งนี้เกิดจากการเติมกราฟีนที่มีความแข็งแรงสูงทำให้เกิดการขัดขวางการเคลื่อนที่ของสายโซ่พอลิเมอร์ อีกทั้งอนุภาคกราฟีนและเบนซอกซาซีนสามารถยึดเหนี่ยวกันเพิ่มสูงขึ้น ในขณะที่ความสามารถในการนำความร้อนของคอมพอสิตมีค่าสูงสุดที่ 14.5 วัตต์ต่อเมตรเคลวิน เมื่อเติมกราฟีนร้อยละ 7.5 โดยน้ำหนัก เนื่องจากระบบคอมพอสิตในงานวิจัยใช้กราไฟท์ขนาดใหญ่ช่วยลดความต้านทานเชิงความร้อน และสามารถเติมสารตัวเติมได้ในปริมาณสูง ขณะที่การเติมกราฟีนจะช่วยเติมเต็มช่องว่างระหว่างอนุภาคกราไฟท์ ทำให้เกิดเป็นโครงข่ายเส้นทางการนำความร้อนที่ดี จึงสามารถนำความร้อนได้สูงขึ้น นอกจากนั้นค่ามอดูลัสภายใต้แรงดัดโค้งและค่าความแข็งแรงภายใต้แรงดัดโค้งของคอมพอสิต มีค่า 16.8 จิกะปาสคาลและ 55 เมกกะปาสคาลตามลำดับ ค่าการดูดซึมน้ำของคอมพอสิตมีค่าประมาณร้อยละ 0.04 ที่เวลา 24 ชั่วโมง และความสามารถในการนำไฟฟ้าของระบบคอมพอสิตที่เติมกราฟีนร้อยละ 7.5 โดยน้ำหนัก มีค่า 323 ซีเมนต์ต่อเซนติเมตร จากผลการทดลองระบบกราไฟท์/กราฟีนคอมพอสิตมีค่าเป็นไปตามมาตรฐานของกรมพลังงานของสหรัฐอเมริกา (DOE) จึงทำให้คอมพอสิตระหว่างพอลิเบนซอกซาซีนกับกราไฟท์/กราฟีนมีความเหมาะสมที่จะนำไปประยุกต์ใช้เป็นแผ่นไบโพลาร์ในเซลล์เชื้อเพลิงชนิดเยื่อแลกเปลี่ยนโปรตอน

ภาควิชา วิศวกรรมเคมี

ลายมือชื่อนิสิต

สาขาวิชา วิศวกรรมเคมี

ลายมือชื่อ อ.ที่ปรึกษาหลัก

ปีการศึกษา 2558

5770274121 : MAJOR CHEMICAL ENGINEERING

KEYWORDS: BIPOLAR PLATES / POLYBENZOXAZINE / FUEL CELLS / GRAPHITE/GRAPHENE

MANLIKA PHUANGNGAMPHAN: Development of Highly Thermally Conductive Graphite/Graphene Filled Polybenzoxazine for Bipolar Plates in Fuel Cells. ADVISOR: ASSOC. PROF. SARAWUT RIMDUSIT, Ph.D., 112 pp.

Development of a suitable and efficient bipolar plate material for polymer electrolyte membrane fuel cell (PEMFC) is scientifically and technically important due to the critical required on higher thermal properties, higher electrical conductivity and better mechanical properties of this material. Therefore, this research emphasizes on the development of highly filled graphite/graphene filled polybenzoxazine composites and investigates thermal conductivity, electrical conductivity and mechanical properties of the obtained composites. Graphite at aggregate size of 240 μm was used in this research. The overall carbon filler content was fixed at 83wt% and varying composition of graphene from 0-10wt% at an expense of the graphite. The experimental results revealed that storage modulus at 25°C of the composites filled with 7.5wt% of graphene content (75.5wt% of graphite) filled in the polybenzoxazine, raised from 5.9 GPa of the neat polybenzoxazine up to about 16.9 GPa in the composites which is about 166% improvement. The glass-transition temperatures (T_g) of our composites were observed to be in the range of 200 to 209°C. The T_g of the composites was found to increase with an increasing graphene contents due to good interfacial interaction between the filler and the matrix which can hinder the polymer chain movement. Moreover, thermal conductivity of the composite filled with 7.5wt% of graphene loading was found to be as high as 14.5 W/mK. This phenomenon suggested that the aggregate graphite provided beneficial in producing a small number of interfaces, thus resulting in a high thermal conductivity in overall. In addition, an incorporation of a small amount of graphene in the composite enhanced the interaction between the graphite by bridging the gaps between them. The flexural modulus and flexural strength of the composites filled with 7.5wt% of graphene were found to be as high as 16.8 GPa and 55 MPa, respectively. Water absorption of graphite/graphene filled polybenzoxazine composite was relatively low with the value of only about 0.04% at 24 hours of immersion. Additionally, electrical conductivity of the composite was measured to be 323 S/cm at 7.5wt% of graphene loading. From the results, the values of thermal conductivity, electrical conductivity, flexural modulus, flexural strength as well as water absorption of graphite/graphene filled polybenzoxazine composites satisfied the use as bipolar plate according to the United States Department of Energy (DOE) requirements. Therefore, these graphite/graphene filled composites based on polybenzoxazine are highly attractive for bipolar plates in PEMFC applications.

Department: Chemical Engineering

Student's Signature

Field of Study: Chemical Engineering

Advisor's Signature

Academic Year: 2015

ACKNOWLEDGEMENTS

The author would like to express my sincerest gratitude and deep appreciation to my advisor, Assoc. Prof. Dr. Sarawut Rimdusit, for his kindness, invaluable supervision, guidance, advice, and encouragement throughout the course of this study.

I also gratefully thank Assoc. Prof. Dr. Siriporn Damrongsakkul, Dr. Paravee Vas-Umnuay and Asst. Prof. Dr. Chanchira Jubslip for their invaluable comments as a thesis committer.

This research is supported by the Ratchadaphisek somphot Endowment Fund (2015) of Chulalongkorn University (CU-58-030-AM) and The Institutional Research Grant (The Thailand Research Fund), IRG 5780014, and Department of Chemical Engineering, Chulalongkorn University, Contract No. RES_57_411_21_076.

In addition, the authors would like to thank Mektec Manufacturing Corporation (Thailand) Limited for the kind support in the use of laser flash apparatus for thermal conductivity measurement.

Additionally, I would like to extend our grateful thanks to all members of Polymer Engineering Laboratory of the Department of Chemical Engineering, Faculty of Engineering, Chulalongkorn University, for their assistance, discussion, and friendly encouragement in solving problems. Finally, my deepest regards to my family, particularly my parents, who have always been the source of my unconditional love, understanding, and generous encouragement during my studies. Also, every person who deserves thanks for encouragement and support that cannot be listed

CONTENTS

	Page
THAI ABSTRACT	iv
ENGLISH ABSTRACT	v
ACKNOWLEDGEMENTS	vi
CONTENTS	vii
LIST OF FIGURES	x
LIST OF TABLES	xiv
CHAPTER I INTRODUCTION.....	1
1.1 General Introduction.....	1
1.2 Objectives	4
1.3 Scopes of the study	5
1.4 Procedure of the study	6
CHAPTER II THEORY	7
2.1 Fuel cells.....	7
2.2 Proton-exchange membrane fuel cell (PEMFC).....	8
2.3 Bipolar plates	13
2.4 Development for bipolar plates	16
2.5 Graphite.....	23
2.6 Graphene.....	28
2.7 Properties of graphene.....	30
2.8 Benzoxazine Resin.....	32
CHAPTER III LITERATURE REVIEWS	36
CHAPTER IV EXPERIMENTAL	48

	Page
4.1 Materials and Monomer Preparation	48
4.1.1 Benzoxazine Monomer Preparation	48
4.1.2 Graphite Characteristics.....	49
4.1.3 Graphene Characteristics.....	49
4.2 Specimen Preparation.....	49
4.3 Characterization Methods	50
4.3.1 Differential Scanning Calorimetry (DSC)	50
4.3.2 Density Measurement.....	50
4.3.3 Dynamic Mechanical Analysis (DMA)	52
4.3.4 Thermogravimetric Analysis (TGA).....	52
4.3.5 Specific Heat Capacity Measurement.....	53
4.3.6 Thermal Diffusion Measurement.....	53
4.3.7 Thermal Conductivity Measurement.....	54
4.3.8 Flexural Properties Measurement.....	54
4.3.9 Water Absorption.....	55
4.3.10 Electrical Conductivity Measurement	56
4.3.11 Scanning Electron Microscope (SEM).....	56
CHAPTER V RESULTS AND DISCUSSION	57
5.1 Graphite-filled Polybenzoxazine Characterization	57
5.1.1 Actual Density and Theoretical Density Determination of Graphite Filled Polybenzoxazine Composites	57
5.2 Graphite/Graphene Filled Polybenzoxazine Characterization.....	58
5.2.1 Curing Behavior of Graphite/Graphene Filled Polybenzoxazine Composites with Curing Condition.....	58

5.2.2 Dynamic Mechanical Properties of Graphite/Graphene Filled Polybenzoxazine Composites.....	61
5.2.3 Effect of Graphene Loading on Thermal Stability of Graphite/Graphene Filled Polybenzoxazine Composites.....	63
5.2.6 Thermal Conductivity of Graphite/Graphene Filled Polybenzoxazine Composites	67
5.2.7 Effect of the Graphene Loading on Flexural Properties of Graphite/Graphene Filled Polybenzoxazine Composites.....	70
5.2.8 Water Absorption of Polybenzoxazine and Graphite/Graphene Filled Polybenzoxazine Composites at Various Graphene Contents.....	72
5.2.9 Electrical Conductivity of Graphite/Graphene Filled Polybenzoxazine at Various Graphene Contents.....	73
5.2.10 SEM Characterization of Graphite/Graphene-Polybenzoxazine	75
CHAPTER VI CONCLUSIONS.....	100
REFERENCES	103
APPENDIX.....	108
APPENDIX A Average graphite aggregate size	109
VITA.....	112

LIST OF FIGURES

	Page
Figure 2.1 Diagram of a PEM fuel cell.	9
Figure 2.2 Fuel cell stack.	10
Figure 2.3 Materials for bipolar plates in fuel cells.	16
Figure 2.4 The crystal structure of perfect graphite, with the unit cell demarcated in bold lines. Also shown are the characteristic lattice parameters at 0 K.	24
Figure 2.5 Sheets of pyrolytic graphite.	24
Figure 2.6 Idealized structure of a single graphene sheet.	29
Figure 2.7 Synthesis route of BA-a-type benzoxazine resin.	33
Figure 2.8 Formation of polybenzoxazine resin network by thermal curing process.	33
Figure 3.1 Thermal conductivity of boron nitride-filled polybenzoxazine as a function of filler contents.	37
Figure 3.2 Thermal conductivity at 25°C of graphite filled polybenzoxazine.	38
Figure 3.3 Effect of the graphite content on electrical conductivity (in-plane) of graphite filled polybenzoxazine composites.	39
Figure 3.4 Effect of the graphene contents on electrical conductivity (in plane)	41
Figure 3.5 Relationship between graphene contents and the flexural properties of graphene-filled polybenzoxazine composites.	42
Figure 3.6 Effect of graphene content on flexural strength of developed composite bipolar plate (CF/CB/(NG+GP)/NPFR 5/5/60/30 vol%).	45

LIST OF FIGURES (Cont.)

	Page
Figure 3.7 Effect of graphene content on in-plane, through-plane electrical conductivity and in-plane thermal conductivity of developed composite bipolar plate (CF/CB/(NG+GP)/NPFR 5/5/60/30 %)	47
Figure 5.1 Theoretical and actual densities of graphite filled polybenzoxazine composites at different sizes of graphite: (●) theoretical density, (■) <50 μm, (●) 140 μm, (▲) 240 μm	77
Figure 5.2 DSC thermograms of graphite/graphene filled benzoxazine molding compound at different graphene contents: (▲) neat polybenzoxazine, (●) 83/0wt%, (▲) 80.5/2.5wt%, (■) 78/5wt%, (◆) 75.5/7.5wt%, (▲) 73/10wt%	79
Figure 5.3 FTIR spectra of as-received graphite grad IG-70 from Toyo tanso, Thailand use in this research.	80
Figure 5.4 FTIR spectra of as-received graphene-grade H from XG Sciences, USA use in this research.	81
Figure 5.5 DSC thermograms of the composite at 2.5wt% of graphene content with various curing times at 200°C, (●) uncured molding compound, (■) 1 hour, (▲) 2 hours, (◆) 3 hours.	82
Figure 5.6 DMA thermograms of graphite/graphene filled benzoxazine molding compound at different graphene contents: (▲) neat polybenzoxazine, (●) 83/0wt%, (▲) 80.5/2.5wt%, (■) 78/5wt%, (◆) 75.5/7.5wt%, (▲) 73/10wt%	83
Figure 5.7 DMA thermograms of graphite/graphene filled benzoxazine molding compound at different graphene contents: (▲) neat polybenzoxazine, (●) 83/0wt%, (▲) 80.5/2.5wt%, (■) 78/5wt%, (◆) 75.5/7.5wt%, (▲) 73/10wt%	84

LIST OF FIGURES (Cont.)

	Page
Figure 5.8 TGA thermograms of graphite/graphene filled benzoxazine molding compound at different graphene contents: (▲) neat polybenzoxazine, (●) 83/0wt%, (▴) 80.5/2.5wt%, (■) 78/5wt%, (◆) 75.5/7.5wt%, (▲) 73/10wt%, (△) neat graphite, (○) neat graphene	85
Figure 5.9 Degradation temperature at 5% weight loss and char yield at 800°C of graphite/graphene filled benzoxazine molding compound at different graphene contents: (●) degradation temperature, (▲) char yield	86
Figure 5.10 Specific heat capacity extrapolated at 25°C of graphite/graphene filled polybenzoxazine as a function of graphene contents.....	88
Figure 5.11 Thermal diffusivity at 25°C of graphite/graphene filled polybenzoxazine as a function of graphene contents.	90
Figure 5.12 Thermal diffusivity of graphite/graphene filled polybenzoxazine composites: (▲) neat polybenzoxazine, (●) 83/0wt%, (▴) 80.5/2.5wt%, (■) 78/5wt%, (◆) 75.5/7.5wt%, (▲) 73/10wt%.....	91
Figure 5.13 Thermal conductivity at 25°C of graphite/graphene filled polybenzoxazine composites as a function of graphene contents.....	93
Figure 5.14 Relation between graphene contents and the flexural modulus of graphite/graphene filled polybenzoxazine composites.	94
Figure 5.15 Relation between graphene contents and the flexural strength of graphite/graphene filled polybenzoxazine composites.	95
Figure 5.16 Water absorption of graphite/graphene filled polybenzoxazine composites: (▲) neat polybenzoxazine, (●) 83/0wt%, (▴) 80.5/2.5wt%, (■) 78/5wt%, (◆) 75.5/7.5wt%, (▲) 73/10wt%.....	96

LIST OF FIGURES (Cont.)

	Page
Figure 5.17 Effect of the graphene contents on electrical conductivity (in-plane) of graphite/graphene filled polybenzoxazine composites.	97
Figure 5.18 SEM micrographs of fracture surface of graphite/graphene filled polybenzoxazine composites:	99



LIST OF TABLES

	Page
Table 2.1 Comparison of operating temperatures, electrolyte materials, charge carriers, efficiencies and application for different types of fuel cell.	7
Table 2.2 U S DOE technical targets for composite bipolar plates.	15
Table 2.3 Comparison between a thermoplastic/filler composite and a thermoset/filler composite for the bipolar plate material.....	21
Table 2.4 Properties of graphite	25
Table 2.5 Properties of graphene.....	29
Table 2.6 Properties of aromatic amines.....	34
Table 2.7 Properties of arylamine-based benzoxazine resin.....	35
Table 3.1 Properties of composite bipolar plate.....	43
Table 5.1 The effect of particle size on composite packing densities.....	78
Table 5.2 Thermal characteristics of polybenzoxazine and graphite/graphene filled polybenzoxazine composites.....	87
Table 5.3 Specific heat capacity values of graphite/graphene filled polybenzoxazine at different graphene contents.	89
Table 5.4 Thermal conductivity of graphite/graphene filled polybenzoxazine composites at 25 ^o C.....	92

CHAPTER I

INTRODUCTION

1.1 General Introduction

The polymer electrolyte membrane fuel cells (PEMFC) have been known as one of the most promising alternative source of energy due to their high efficiency, high power density, and low operation temperature ranging from 60 to 80 °C. The PEMFC converts the chemical energy of the fuel to electrical energy directly so that no pollutant release will be produced. Heat and water will be only byproducts [1].

Bipolar plates are major components of the PEMFC stack, and they account for most of the total weight as well as the main cost of the product. In a typical production, total weight of bipolar plate is around 80% while they are responsible approximately 50% of the total production cost [2]. The main functions of bipolar plate include distributing reactants uniformly and removing heat within active areas, carrying current from cells, preventing leakage of reactants and coolants [3]. As a consequence, bipolar plate in fuel cells should have high electrical and thermal conductivity, sufficient mechanical characteristics, good corrosion resistance, and low gas permeability. Moreover, the bipolar plates need to be lightweight and low cost [2]. Currently technical specification regarding commercial applications are identified and defined by Department of Energy (DOE) of the USA. Technical targets of bipolar

plates for the year 2015 are flexural strength > 25 MPa, electrical conductivity > 100 S/cm, thermal conductivity > 20 W/mK and weight < 0.4 kg/kW [4].

The most commonly material used for manufacture of bipolar plate is graphite due to its superior corrosion resistance, high thermal conductivity, chemical stability, and low density [5]. However, the thickness of the graphite bipolar plate cannot be reduced due to its brittleness and high cost of materials [5, 6]. In the past, several metallic materials have considered as potential as material for bipolar plate production because of its low gas permeability, excellent electrical and mechanical properties. One disadvantage of metallic bipolar plate is corrosiveness thus requires coating for protecting metallic materials which results in greater cost of production. Therefore metallic material would not be considered as ideal material for bipolar plate manufacture [6]. To solve this problem, polymer composite bipolar plates have been developed in order to substitute the use of graphite plates and metallic plates. However, the main disadvantages of graphite-polymer composites are their low electrical conductivity, low thermal conductivity and low mechanical properties. Therefore, an enhancement of electrical, thermal and mechanical properties of composite materials is developed by reinforced with other types of carbon fillers [7].

Theoretically, the highly thermal conductivity depends on conductive network and minimizing thermal resistant. The maximum packing of the filler in the matrix is one way to convince the formation of near-perfect conductive networks. To

achieve high packing density of composites, large particles size are used [8]. Therefore, large graphite size highly filled in composite could lead to the formation of conductive paths network. However, the composites filled with large graphite size have low mechanical properties.

Recently, graphene has attracted both academic and industrial interest, because it can produce a dramatic improvement in properties at very low filler content. Graphene, two-dimensional (2-D) sheet composed of sp^2 carbon atoms arranged in a honeycomb structure, has been explored to be an excellent material due to it has very good mechanical strength (Young's modulus of 1 TPa, ultimate strength of 130 GPa), large specific area (theoretical limit: $2630 \text{ m}^2/\text{g}$), good corrosion resistant and low gas permeability. Especially, its highest electrical conductivity ($>6000 \text{ S/cm}$) and high thermal conductivity (5000 W/mK) thus gains much attention for bipolar plate utilization. Therefore, graphene was used to improve properties of the graphite filled composite [9].

Thermosetting polymers are most commonly used resins in manufacture of various types of composites due to their low viscosity and have high percentage of conductive filler compares to those of thermoplastic polymers. Benzoxazine resins are novel kind of thermosetting phenolic based adhesion that can be synthesized from formaldehyde, phenol, and amine groups. Polybenzoxazines have many attractive properties such as no catalyst of curing require upon curing, no by-product

release during curing, high thermal stability, good mechanical strength and modulus, low dielectric constant, good adhesive properties, high resistance to burning and chemicals. Particularly, benzoxazine resins provide a very low melt viscosity thus facilitate wetting ability to produce highly filled composite. .

The objectives of this work are to prepare the highly filled system of graphite/graphene in polybenzoxazine composites and investigate the influence of graphite/graphene contents on physical, mechanical, electrical, and thermal properties of graphite/graphene in polybenzoxazine composites for an application as bipolar plates in fuel cells.

1.2 Objectives

1.2.1 To investigate effect of graphite particle sizes on maximum packing density of graphite filled polybenzoxazine composites for bipolar plates in PEM fuel cells application.

1.2.2 To investigate effect of graphite/graphene mixing ratios filled polybenzoxazine on physical, electrical, thermal and mechanical properties of resulting composite bipolar plates.

1.3 Scopes of the study

- 1.3.1 Synthesis of benzoxazine resin by solventless technology.
- 1.3.2 Determination of the different graphite size (<50, 140, 240 μm) by varying compositions of graphite at 70wt%, 75wt%, 80wt%,..., maximum packing density.
- 1.3.3 Investigation of graphite/graphene mixing ratios filled benzoxazine resin.
- 1.3.4 Investigation of physical, electrical, thermal and mechanical properties of graphite/graphene based polybenzoxazine composites as follows:
 - Dynamic mechanical analysis (DMA)
 - Blending test (Universal testing machine)
 - Differential scanning calorimetry (DSC)
 - Thermogravimetric analysis (TGA)
 - Thermal conductivity measurement
 - Electrical conductivity measurement
 - Density measurement
 - Surface morphology (Scanning Electron Microscope)

1.4 Procedure of the study

1.4.1 Reviewing related literatures.

1.4.2 Preparation of chemicals and equipment for using in this research such as Graphene, Graphite, Bisphenol-A, Formaldehyde, Aniline etc.

1.4.3 Synthesis of benzoxazine resins (BA-a).

1.4.4 Determination of the different graphite average aggregate size (<50, 140, 240 μm) by Laser particle size and varying compositions of graphite at 70wt%, 75wt%, 80wt%,..., maximum packing density.

1.4.5 Investigation graphite/graphene mixing ratios filled benzoxazine resin.

1.4.6 Determination the physical, mechanical, electrical and thermal properties of the graphite/graphene filled composites based on benzoxazine resin as follows

Physical properties

- Density
- Water absorption
- Scanning Electron Microscope (SEM)
- Laser size particle

Mechanical properties

- Flexural modulus
- Flexural strength

Thermal properties

- Glass transition temperature
- Thermal degradation
- Thermal conductivity

Electrical properties

- Electrical conductivity

1.4.7 Analyze and conclude the experimental results.

1.4.8 Preparation of the final report

CHAPTER II

THEORY

2.1 Fuel cells

Fuel cells are a highly efficient way to use diverse energy sources. Fuel cells can convert chemical energy to direct usable electrical energy with high efficiency without any need of combustion. Therefore, the main benefit of fuel cells is to reduce global carbon dioxide (CO₂). There are many types of fuel cell each operating at various fuels with different electrolyte, and operated at different temperatures operation [10].

Table 2.1 Comparison of operating temperatures, electrolyte materials, charge carriers, efficiencies and application for different types of fuel cell [4, 11].

Fuel Cell	Operating Temperature (°C)	Electrolyte Material	Charge Carrier	Efficiency (Typical)	Applications
DMFC	50-90	Sulphonated PTFE	H ⁺	40%	Portable Power
PEMFC	80	Sulphonated PTFE	H ⁺	40-50%	Distributed power Portable power Transportation
AFC	60-220	Potassium Hydroxide	OH ⁻	50%	Portable Power Backup Power
PAFC	200	Concentrated Phosphoric Acid	H ⁺	40%	Distributed power Transportation
MCFC	650	Molten Carbonate	CO ₃ ²⁻	45-55%	Distributed power
SOFC	600-1000	Yttrium-stabilised Zirkondioxide	O ⁻	50-60%	Electric utility Distributed power

2.2 Proton-exchange membrane fuel cell (PEMFC)

The PEMFCs have received considerable attention for transportation and combined heat and power applications because they have a faster start up time than those of other fuel cells, high power densities, and operate at relatively low temperatures. Moreover, PEMFC represent a clean power source for wide power ranges. Instead of releasing thermal energy by the direct combustion of hydrogen and oxygen, PEMFCs generate energy due to the electrochemical reaction between hydrogen and oxygen.

The anode side of the fuel cell is fed with a stream of hydrogen, which will be divided into protons and electrons in the presence of a catalyst layer. The chemical reaction in this section of the fuel cell is represented by



The protons formed in this reaction permeate through the polymer electrolyte membrane to the cathode of the fuel cell, while the electrons are conducted to an external circuit to power an electric load and then return to the cathode side.

At the bipolar plate in the cathode side, oxygen is feed to the fuel cell, which reacts with the protons flowing through the membrane and the electrons returning

through the external circuit to produce water. The chemical reaction in this section of the fuel cell is represented by



As we can be seen, the overall reaction of PEMFC is given by

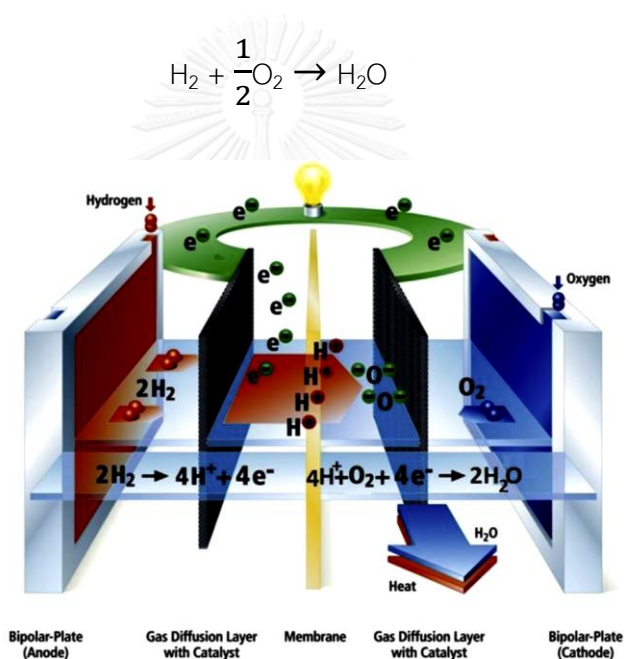


Figure 2.1 Diagram of a PEM fuel cell [5].

2.2.1 PEMFC Components [11-14]

A single fuel cell is only able to produce a certain voltage and current. In order to obtain a higher voltage and current or power, fuel cells are connected in either series or parallel, called stacks, see Figure 2.2 Individual cells communicate in

many ways in a stack such as electrical connection, through flow field, heat transfer connection. The number of individual cells contained within one stack is typically greater than 50 and varies significantly with stack design [13].

Each cell in the stack is made up of a polymer electrolyte and porous electrodes. In a stack the cells are connected alternately in series with bipolar plates that also serve to deliver reactant gases, remove exhaust gases and liquid water and provide cooling if required [12].

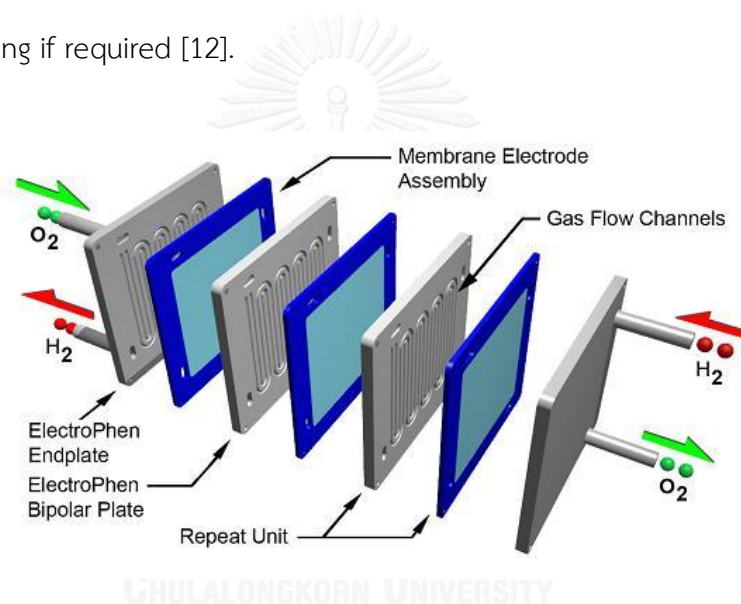


Figure 2.2 Fuel cell stack [14].

2.2.2.1 Gas Diffusion Layer

The gas diffusion layer (GDL) is a porous material. The GDL allows reactant gases to pass through it to the catalyst layer. The transport of electrons to the external circuit is facilitated since carbon is one of conductive material. The GDL can be fabricated with either carbon cloth or carbon paper. The carbon material used for

fabricating the GDL can be treated with tetrafluoroethylene. Thus, the carbon material becoming a hydrophobic material can prevent the GDLs from flooding, while still allowing gases and steam to flow through the pores of the carbon paper.

In addition to these requirements, the gas diffusion layer must have the following characteristic.

- Must have good thermal and electrical conductivity in two directions, through-plane and in-plane directions.
- The pores' size of the GDL face adjacent to the catalyst layer must not be too large.
- The GDL must be rigid to support the MEA. Moreover it must be flexible to maintain good electrical contacts [12].

2.2.2.2 Electrolyte Membrane

The polymer electrolyte membrane in a PEMFC should have high proton conductivity, while also acting like a barrier to avoid the fuel mixing with the reactant gases. It must be made from materials which are chemically and mechanically stable in the fuel cell operating conditions. The common materials used as membranes for PEMFCs are perfluorocarbon-sulfonic acid ionomer and Nafion™, the latter being produced by Dupont. The use of a solid electrolyte membrane represents more advantage when compared with systems using a liquid electrolyte.

The electrolyte membrane used in PEMFCs is a proton-conducting membrane cast in solid polymer form. Solid electrolyte offers a series of advantages as compared with systems using liquid electrolyte such as AFCs and PAFCs [12].

2.2.2.3 Catalyst layers

The catalyst layer, between the gas diffusion layer and the polymer electrolyte membranes, is a layer which the hydrogen is being split into protons and electrons in anode chamber and which the water is being produced in the cathode side of the fuel cell. The electrochemical reactions occur in a section of the catalyst layer which the three chemical species (protons, electrons and reactant gases) involved have access. Recently, PEMFCs technologies use platinum as the most common material for catalyst layers. The thickness of this layer should be minimized in order to prevent the voltage drops due to the proton transport and permeation of reactant gases in the depth of the catalyst layer [12].

2.2.2.4 Bipolar Plates

Bipolar plates are the component of a PEM fuel cell stack. The bipolar plates are represented the most significant part by weight, volume and cost. Bipolar plates receive this name since they are conductive plates which act as anode for one cell and as cathode for the adjacent cell. There are different materials used for bipolar plates, such as metal, carbon or conductive polymer composites [12].

2.3 Bipolar plates

Bipolar plates are main components of PEMFC stack. In a typical stack, the bipolar plates account over 80% of the overall mass and almost all of the volume. Bipolar plates have a higher cost compared to the other fuel cell components due to lengthy production cycles for machining and surface treatment as most bipolar plates are made from graphite or stainless steel [11, 12, 15].

The bipolar plate performs a number of functions within the PEMFC as described below.

1. Providing a physical barrier to avoid mixing of the oxygen, fuel and coolant fluids
2. Separating fuel and oxygen and feeding H_2 to the anode and O_2 to the cathode, while removing product water and un-reacted gases.
3. Providing a gas flow field channels are etched into the side of the plate next to the backing layer to carry the reactant gases from the place where it enters the fuel cell to the place where it exits.
4. Conducting electrons to complete the circuit, including by collecting and transporting electrons from the anode and cathode, as well as, connecting individual fuel cells in series to form a fuel cell stack of the required voltage (i.e., fuel cells are typically arranged in a bipolar configuration)

5. Providing thermal conduction to help regulate fuel cell temperature and removing heat from the electrode to the cooling channels.
6. Providing mechanical strength and rigidity to support the thin membrane and electrodes and clamping forces for the stack assembly.
7. Light weight for comfortable to use in portable application and transportation.

The materials of the bipolar plate must have particular properties because of its multiple responsibilities. Properties of materials, which chosen to bipolar plate must be considered for achievable design for a fuel cell application. To perform these functions, the material used for bipolar plates must have the following characteristics [12].

- Impermeable to reactant gases (hydrogen and oxygen from air in PEMFCs)
- Good electrical and thermal conductivity
- A balance between conductivity, strength, size and weight. Weight becomes a priority when fuel cells are to be used for transport and mobile devices.
- Resistance to corrosion
- Easy to manufacture in large quantities
- The distribution of the reactant gases in the channels must be uniform to increase efficiency of the stack.

An ideal material should combine the following characteristics that are defined by Department of Energy (DOE) as shown in table 2.2.

Table 2.2 U S DOE technical targets for composite bipolar plates. [4, 11]

Technical Targets: Bipolar plates			
Characteristic	Units	2010 Target	2015 Target
Electrical conductivity	S/cm	>100	>100
Thermal conductivity	W/mK	>10	>20
Flexural strength	MPa	>25	>25
Hydrogen permeation rate	Std cm ³ /sec cm ² Pa @ 80 °C, 3 atm 100% RH	<2×10 ⁻⁶	<2×10 ⁻⁶
Weight	Kg/kW	<0.4	<0.4
Cost	\$/kW	5	3

2.4 Development for bipolar plates

Several types of materials are currently used in bipolar plates. The materials investigated so far can be broadly classified as

1. Non-metal: non-porous graphite/electrographite.
2. Metals: non-coated and coated.
3. Composites: polymer-carbon and polymer-metal.

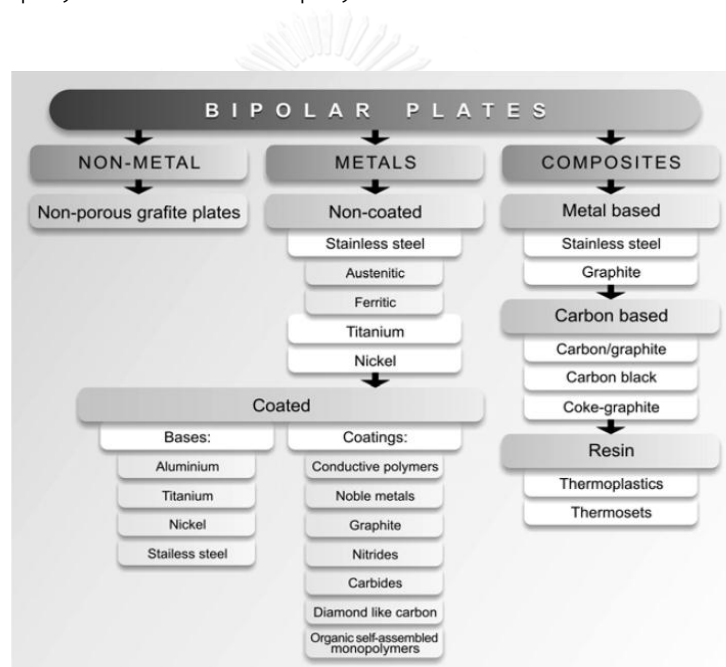


Figure 2.3 Materials for bipolar plates in fuel cells [16].

2.4.1. Non-Porous Graphite Bipolar Plates [17-20]

In the past, the most commonly used materials for bipolar plates in the proton exchange membrane is graphite due to excellent chemical stability to survive the fuel cell environment, excellent resistance to corrosion, low bulk resistivity, low

specific density, and low electrical contact resistance with electrode backing materials. This low contact resistance results in high electrochemical power output. The disadvantages of graphite plates are difficulties in machining, and its brittleness due to which bipolar plate requires a thickness of the order of several millimeters. Bipolar plates have traditionally been created from graphitic carbon impregnated with a resin or subject to pyrolytic impregnation. A thermal treatment is used in the process to seal the pores. This seal renders the bipolar plates impermeable to fuel and oxygen gases. This type of bipolar plate is available in the fuel cell market from the likes of POCO Graphite and SGL Carbon. Due to the brittle nature of graphite, graphite plates used in fuel cell stacks must typically be several millimeters thick, which add to the volume and weight of the stack.

In order to solve this problem, flexible graphite was considered the material of choice for bipolar plates in PEMFC. Flexible graphite is made from a polymer/graphite composite, in which the polymer acts as a binder. The graphite principally used for the composite is expanded graphite (EG), produced from graphite flakes intercalated with highly concentrated acid. The flakes can be expanded up to a few hundred times their initial volume. The expansion leads to a separation of the graphite sheets into nano-platelets with a very high aspect ratio. This layered structure gives higher electrical and thermal conductivity. The expanded form is then compressed to the desired density and pressed to form the bipolar plate. In

comparison to conventional graphite bipolar plates, the bipolar plates produced from EG are thinner.

2.4.2 Metallic Bipolar Plates [17, 21, 22]

Metal is also a good material for bipolar plates. The advantages of metal are good electrical conductivity, excellent mechanical properties, gas impermeability and ease of fabrication, but low corrosion resistance. Corrosion of the metal bipolar plate leads to a release of multivalent cations, which can lead to an increase in membrane resistance and to the poisoning of the electrode catalyst. The most important benefit is that the resultant stack can be smaller and lighter than graphite bipolar plates. Two advantages to metallic plates that they can be stamped to accommodate flow channels and that the resultant plate can be varied thick, for example 100 μm . However, the main disadvantage of metal plates is their susceptibility to corrosion and dissolution in the fuel cell operating environment of 80°C. To solve these issues, researchers have considered of non-coated metal alloys, precious non-coated metals, and coated metals with a protective layer. Metals investigated include aluminum, stainless steel, titanium and nickel. Titanium offers excellent electrical performance and power densities, but it is expensive and requires precious metal coatings for durability.

Non-coated

Stainless steels (SSs) are the only material in this category to have received considerable attention due to their relatively high strength, high chemical stability, low gas permeability, wide range of alloy choice, and applicability to mass production and low cost. Major concerns have been extent of corrosion (and its products) and the contact resistance of the surface passivation film. Candidate SSs have been tested and used as BPs by different authors, the result showed that corrosion rate is low and PEM cell output is stable for thousands of hours [18].

Coated

Aluminum, stainless steel, titanium and nickel are considered as possible alternative materials for BP in PEM fuel cells. To avoid corrosion, metallic BPs are coated with protective coating layers. Coatings should be conductive and adhere to the base metal without exposing it. Further the coefficient of thermal expansion of the base metal and the coating should be as close as possible to eliminate the formation of micro-pores and micro-cracks in coatings due to unequal expansion. Two types of coatings, carbon-based and metal-based, have been investigated. Carbon-based coatings include graphite, conductive polymer, diamond-like carbon and organic self-assembled monopolymers. Noble metals, metal nitrides and metal carbides are some of the metal-based coatings [17].

2.4.3 Composite Bipolar Plate [20, 23, 24]

Composite bipolar plates are an attractive option for proton exchange membrane fuel cells use. They not only offer the advantage of low cost, lower weight and greater ease of manufacture than traditional graphite but also their properties can be tailored by changing different reinforcements and the resin systems. Two different types of resins are used to fabricate composite plates are thermoplastic and thermosetting. The polymer matrix used to bind the fillers also influences the electrical behavior of the composite. Furthermore, the type of polymer determines the processing method of bipolar plates and their recyclability. Both thermoplastic and thermosetting resins may be selected, depending on the criteria adopted by the designer. Thermoplastics based bipolar plates are fully recyclable. However, before being removed from the mold, they must solidify to achieve suitable mechanical strength. This is carried out from a cooling step that increases the production cycle of a single component. Thermosets, on the other hand, are not recyclable after curing in the mold. However, once cured through the action of pressure and heat, they do not need to be cooled before being removed from the mold. As a result, the production cycle is faster than that of thermoplastics, as the cooling step is eliminated. Therefore, the manufacturing cost of thermosets based composite bipolar plates is diminished.

Table 2.3 Comparison between a thermoplastic/filler composite and a thermoset/filler composite for the bipolar plate material [24].

	Thermoset/filler composites	Thermoplastic/filler composites
Advantage	<ul style="list-style-type: none"> -Higher temperature operation than thermoplastic -Fast cycle-time -Flow-field introduced during moulding -Low contact resistance 	<ul style="list-style-type: none"> - Injection moulding lends itself to manufacturing automation - Fast cycle-time - Flow-field introduced during moulding - Low contact resistance
Disadvantage	<ul style="list-style-type: none"> -Relatively low electrical conductivity 	<ul style="list-style-type: none"> - Low electrical conductivity when using standard thermoplastics - Limited to low-temperature operation - Injection moulding difficult at high filler loading - Generally less chemically stable than thermoset resin-
Processing option	<ul style="list-style-type: none"> -Compression moulding -Post-moulding CNC milling of blank 	<ul style="list-style-type: none"> - Injection moulding - Compression moulding - Post-moulding CNC milling of blank

Metal-based Bipolar Plates

Metal-based bipolar plates are made of multiple materials, such as stainless steel, plastic, or porous graphite, so that the benefits of different materials can be harvested in a single bipolar plate. One of the main advantages of porous graphite bipolar plates is the production low cost. Los Alamos National Laboratory has developed a metal based composite bipolar plate based on porous graphite, polycarbonate plastic and stainless steel. Stainless steel also provides rigidity to the

structure while the graphite resists corrosion. The polycarbonate provides chemical resistance and can be molded to any shape to provide for gaskets and manifolding. The layered plate appears to be a very good alternative from stability and cost standpoints.

Carbon-based Bipolar Plates

Carbon-polymer composites are created by incorporating a carbonaceous material into a polymer binder. The preference for the polymer binder is governed by the chemical compatibility with the fuel-cell environment, mechanical and thermal stability, processability when loaded with conductive filler, and cost. Two different main types of resins are used to fabricate composite plates: thermoplastic and thermosetting. Among the thermosetting resins, such as phenolics, epoxies, polyester, and vinyl ester, etc., the epoxy resin is a popular choice for carbon-polymer bipolar plate production. The thermosetting resins have low viscosity, and thereby contain a higher proportion of conductive fillers. During the molding process, the thermosetting resin allows for molding of intricate details. Moreover, the resins can be highly cross-linked through a proper curing process, and the cross-linked structure gives good chemical resistance.

2.5 Graphite

There are four forms of crystalline carbon such as carbon nanotubes, diamonds, fullerenes, and graphite. The origin of the word "graphite" is the Greek word "graphein" which means "to write". Indeed, graphite has been used to write (and draw) since the dawn of history and the first pencils were manufactured in England in the 15th century. In the 18th century, it was demonstrated that graphite actually is an allotrope of carbon [25]. The intercalation of graphite compounds are formed by insertion of atomic or molecular layers of a different chemical species called the intercalate between layers in a graphite host material. Figure 2.4 shows the structure of graphite a semi-metallic allotrope of carbon. Graphite features hexagonal ABAB stacking with an interlinear gap that is sufficiently large to permit only Van der Waals interactions between atoms occupying different planes. The covalent bonds exist within each plane, and the exceptionally large cohesive energy of 7.37 eV is primarily responsible for the high melting temperature of graphite. Conductivity of graphite is dependent on crystallographic direction, with a high in-plane conductivity arising from the presence of de-localized electrons. These electrons are further responsible for graphite is dull. Properties of graphite are shown in Table 2.4. [26].

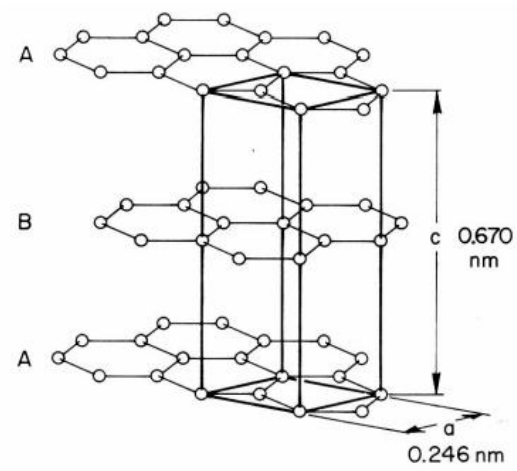


Figure 2.4 The crystal structure of perfect graphite, with the unit cell demarcated in bold lines. Also shown are the characteristic lattice parameters at 0 K [27].

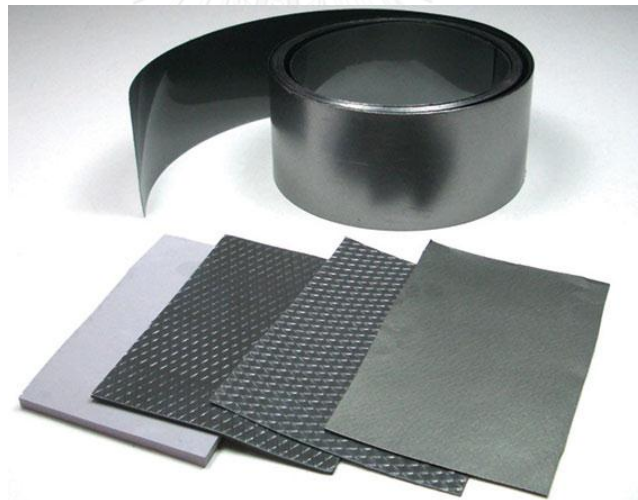


Figure 2.5 Sheets of pyrolytic graphite [27].

Table 2.4 Properties of graphite [28].

Properties	Units	Test	Value
Physical			
Chemical Formula	-	-	C
Density, ρ	g/cm ³	ASTM C20	2.25
Color	-	-	black
Crystal Structure	-	-	hexagonal
Water Absorption	%	ASTM C373	0.5 - 3.0
Hardness	Moh's	-	1.0 - 1.5
Hardness	Knoop (kg/mm ²)	Knoop 100g	-
Mechanical			
Compressive Strength	MPa	ASTM C773	96
Tensile Strength	MPa	ACMA Test #4	4.8
Modulus of Elasticity (Young's Mod.)	GPa	ASTM C848	4.8
Flexural Strength (MOR)	MPa	ASTM F417	50
Thermal			
Max. Use Temperature	°C	No load cond.	3650
Thermal Shock Resistance	DT (°C)	Quenching	200 - 250
Thermal Conductivity	W/mK	ASTM C408	100~400 (on plane)
Coefficient of Linear Thermal Expansion, α_l	mm/m°C (~25°C through ±1000°C)	ASTM C372	8.39
Specific Heat, c_p	cal/g°C	ASTM C351	0.16
Electrical			
Electrical Resistivity	Wcm	ASTM D1829	7×10^{-3}

The unique properties of graphite resulting from its distinctive layered structure and chemical inertness make it be used in many applications:

- Good electrical conductivity: the temperature coefficient of electrical resistance of graphite is negative in a certain range of temperature, unlike that of metals. Near absolute zero, graphite has only a few free electrons and acts as an insulator. When temperature rises, electrical conductivity increases
- Good thermal conductivity: outstanding heat transfer properties
- Unique mechanical strength: the tensile, compressive and flexural strength of graphite increases as temperature increases to 2700 K. At 2700 K, the strength of graphite is double it has when at room temperature.
- Low coefficient of thermal expansion
- High thermal shock resistance: rapid heating or cooling is not a problem
- Graphite is not wetted by molten glass or by most molten metals
- Low friction's coefficient
- High chemical resistance
- Corrosion resistance: oxidation resistance in air up to 500°C
- Low capture cross-section for neutrons
- Problem-free machining with standard machine tools: graphite can be machined easily. Complicated parts with close tolerances can be machined with precision

- Reasonable cheap material compare with other material with similar corrosion resistance
- Graphite does not melt but sublimates at about 3900 K. In air, graphite is resistant to oxidation up to 750 K.
- Graphite displays extremely low creep at room temperature, its flow characteristics being comparable to those of concrete. Creep in graphite is strongly dependent on the grain orientation (creep is defined as plastic flow under constant stress).

Graphite is inert behavior toward most chemicals and high melting point make it an ideal material for use in many manufactures such as the steel manufacturing process, refractory linings in electric furnaces, containment vessels for carrying molten steel throughout manufacturing plants, and casting ware to create a shaped end-product. Moreover, graphite is used as a foundry dressing, which assists in separating a cast object from its mould following the cooling of hot metal. The automotive industry uses graphite extensively in the manufacture of brake linings and shoes. Graphite is an effective lubricant over a wide range of temperatures and can be applied in the form of a dry powder or as a colloidal mixture in water or oil. Other uses include electrodes in batteries, brushes for electric motors, and moderators in nuclear reactors [29].

2.6 Graphene

Graphene is a fascinating material with many potential properties. In 2004, graphene is discovered by Prof. Andre Geim and Prof. Konstantin Novoselov at the University of Manchester. Graphene is single layer sheet of a two-dimension sp^2 bonded carbon atoms arranged in a honeycomb crystal lattice. Graphene is basic structural unit which can form many structural of carbon nanofiller such as wrapped to form 0-D fullerenes rolled to form 1-D carbon nanotubes, stacked to form 3-D graphite. The length of carbon-carbon bond in graphene is about 0.142 nanometers. The graphene layer thickness ranges from 35 to 1 nanometers. Graphene is the strongest material with Young's Modulus of 1 TPa and ultimate strength of 130 GPa. It has very high electrical conductivity (>6000 S/cm), thermal conductivity (5000 W/mK), surface area (2630 m²/g), elasticity and gas impermeability [9]. Since graphene can be mixed with polymer to make composites which good physical properties. Therefore, graphene has a potential for improving mechanical, thermal, electrical and gas barrier properties of polymer composites.

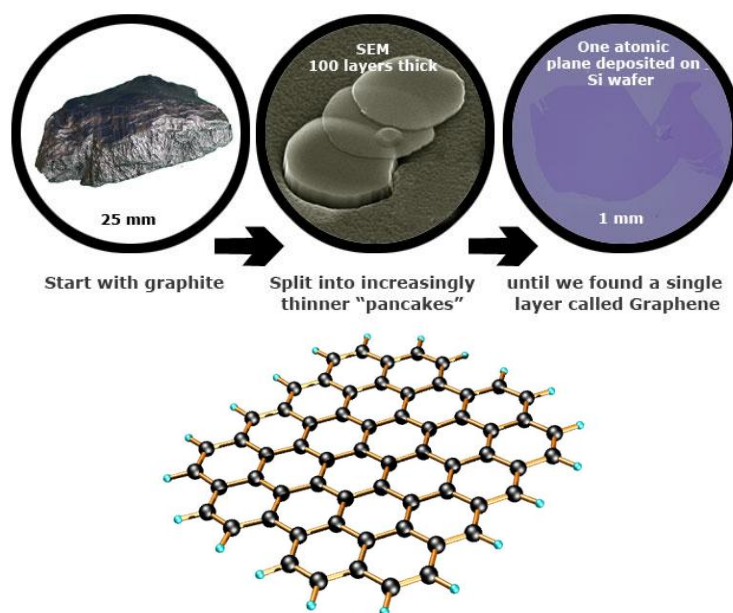


Figure 2.6 Idealized structure of a single graphene sheet [30]

Table 2.5 Properties of graphene [9]

Properties	Values
Physical properties	
Chemical formula	C
Color	Black
Crystal structure	Hexagonal
Density (ρ)	2.2 g/cm ³
Carbon-carbon bond length	0.142 nm
Thickness	35-1 nm
Extremely high surface area	2630 m ² /g
Electrical properties	
Electrical conductivity	> 6000 S/cm
Thermal properties	
Thermal conductivity	5000 W/mK in-plane
Low coefficient of thermal expansion	1×10 ⁻⁶ K ⁻¹
Mechanical properties	
Mechanical properties	Young's modulus (1 TPa), Ultimate strength (130 GPa)

2.7 Properties of graphene

Electronic Properties

The electronic properties of graphene are also highly unusual. Graphene is a great conductor; First off, the electrons are faster and much more mobile, which opens up the possibility of computer chips that work more quickly with less power than the ones we use today. Second, the electrons move through graphene a bit like photons (wave-like particles of light), at speeds close enough to the speed of light as fast as just one hundredth that of the speed of light. [30-32].

Thermal and thermoelectric properties

Graphene is a perfect thermal conductor. Its thermal conductivity was measured recently at room temperature and it is much higher than the value observed in all the other carbon structures as carbon nanotubes, graphite and diamond ($> 5000 \text{ W/mK}$). The ballistic thermal conductance of graphene is isotropic, i.e. same in all directions. Similarly to all the other physical properties of this material, its 2-D structure makes it particularly special. Graphite, the 3-D version of graphene, shows a thermal conductivity about 5 times smaller (1000 W/mK). The phenomenon is governed by the presence of elastic waves propagating in the graphene lattice, called phonons.

The study of thermal conductivity in graphene may have important implications in graphene-based electronic devices. As devices continue to shrink and

circuit density increases, high thermal conductivity, which is essential for dissipating heat efficiently to keep electronics cool, plays an increasingly larger role in device reliability.

Mechanical properties

To calculate the strength of graphene, scientists used a technique called Atomic Force Microscopy. By pressing graphene that was lying on top of circular walls, they measured just how far you can push graphene with a small tip without breaking it. The result shows that graphene is harder than diamond and about 300 times harder than steel. The tensile strength of graphene exceeds 1 TPa.

However graphene is so strong. Graphene can be stretched up to 20% of its initial length. It is expected that graphene's mechanical properties will find applications into making a new generation of super strong composite materials and along combined with its optical properties, making flexible displays.

Optical properties

Graphene, despite being the thinnest material only one atom thick, is still visible to the naked eye. Graphene is almost completely transparent; in fact, graphene transmits about 97–98 percent of light (compared to about 80–90 percent for a basic, single pane of window glass). It absorbs a high 2.3% of light that passes through it, which is enough that you can see it in air. So that, graphene is also an amazing conductor of electricity such as solar panels, LCDs, and touchscreens. A

material than combines amazing transparency, superb electrical conductivity, and high strength.

Impermeability

Sheets of graphene have such closely knit carbon atoms that they can work like super-fine atomic nets, stopping other materials from getting through. That means graphene is useful for trapping and detecting gases but it might also have promising applications holding gases (such as hydrogen) that leak relatively easily from conventional containers. One of the drawbacks of using hydrogen as a fuel (in electric cars) is the difficulty of storing it safely. Graphenes, potentially, could help to make fuel-cell cars running on hydrogen a more viable prospect.

2.8 Benzoxazine Resin

Polybenzoxazine is a newly developed class of thermosetting resins. Polybenzoxazine is a phenolic polymer which generated from phenol, formaldehyde and amine. The benzoxazine resin is synthesized from the reaction of bisphenol-A, paraformaldehyde and aniline at 1:4:2 mole ratio at 110°C without the use of any solvent follow by Ishida in 1996 [33]. This solventless synthesis is a convenient method for preparation of benzoxazine monomer series. The synthesis of monomer is shown in Figure 2.7. The obtained benzoxazine resin can be polymerized by ring-opening polymerization of cyclic monomers via thermal cure without an addition of any catalyst or curing agent. The structural change in benzoxazine monomer to polybenzoxazine via thermal polymerization is shown in Figure 2.8

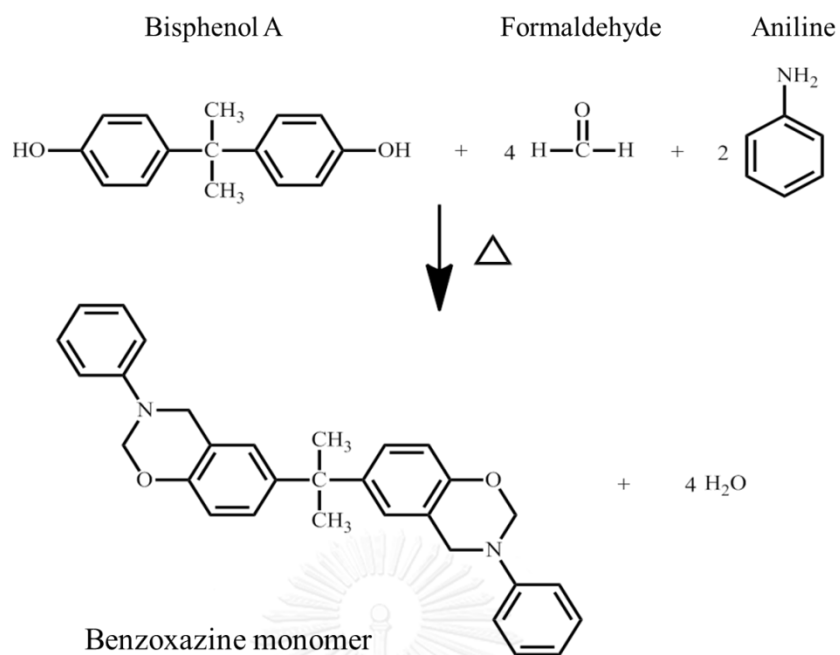


Figure 2.7 Synthesis route of BA-a-type benzoxazine resin [10]

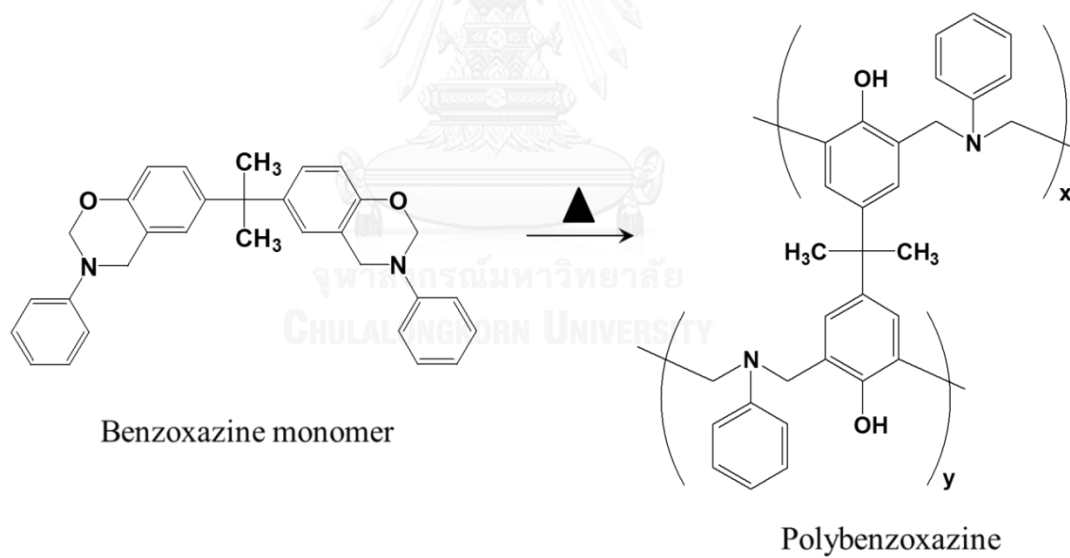


Figure 2.8 Formation of polybenzoxazine resin network by thermal curing process

[10]

The polybenzoxazine have excellent thermal, mechanical, electrical, chemical and physical properties such as high moduli, high glass-transition temperature, high char yield, near-zero volumetric shrinkage upon polymerization, low water absorption, low melt viscosity, excellent resistance to chemicals and UV light, and no by-product during cure. The other advantages of polybenzoxazine include easy processing ability, lack of volatile formation, all attractive for composite material manufacturing. Furthermore, benzoxazine resin is able to be alloyed with several other polymer or resins. In the literature reported that the mixture of the benzoxazine resin with bisphenol-A typed epoxy which the addition of epoxy to the polybenzoxazine network greatly increases the crosslink density of the thermosetting matrix and strongly influences its mechanical properties.

Table 2.6 Properties of aromatic amines [34]

Properties	Aniline
Molecular weight (g/mol)	93.127
Melting point (°C)	-6.02
Boiling point (°C)	184.17
Density (g/cm ³)	1.0217

Table 2.7 Properties of arylamine-based benzoxazine resin [35]

Properties	BA-a
T _g (DSC)	168
Char yield (% at 800°C)	30
Td at 5% wt. loss (°C)	315
Storage modulus at 28°C (GPa)	1.39
Loss modulus at 28°C (MPa)	15.7
Crosslink density (mol/cm ³)	1.1x10 ⁻³

In this research, we use benzoxazine resins which will be synthesized from bisphenol-A, formaldehyde and aromatic amine-based (aniline). Properties of these aromatic amines (arylamines) are shown in Table 2.6 and Table 2.7 show properties of arylamine-based benzoxazine resins.

CHAPTER III

LITERATURE REVIEWS

H. Ishida and S. Rimdusit (1998) [8] developed highly thermally conductive boron nitride filled polybenzoxazine composites. The result in figure 3.1 shown that the composite can be produced with a remarkably high value of thermal conductivity of 32.5 W/mK at 78.5% by volume or 88% by weight of boron nitride filler. The conductive networks of the large particle size are formed, the thermal conductivity of the composites will exceed that of the smaller particles as the formation of the conductive paths of the large particles renders less thermal resistance along the paths. The phenomenon is more pronounced at the filler content exceeding the maximum packing of smaller particles, since the maximum packing of smaller particle size is less than the maximum packing of the larger particles. Moreover, the very low melt viscosity and good adhesion of benzoxazine resin results in its ease of filler mixing during the molding compound preparation thus giving its outstanding thermal conductivity.

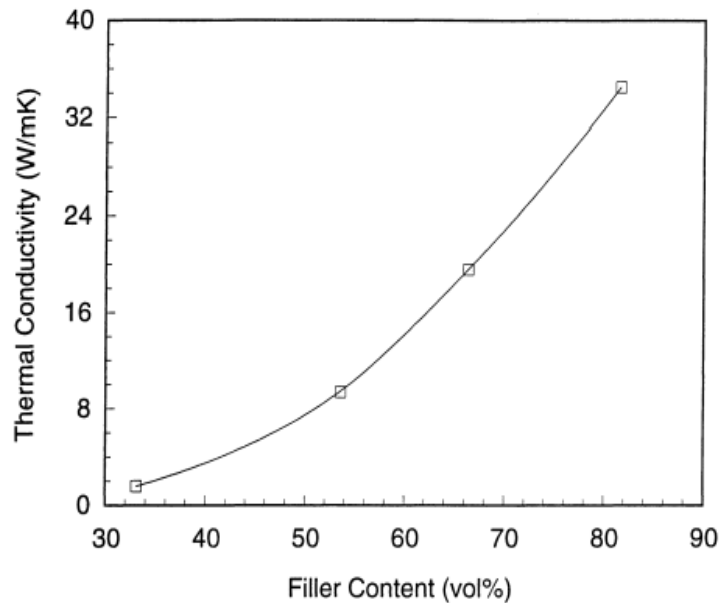


Figure 3.1 Thermal conductivity of boron nitride-filled polybenzoxazine as a function of filler contents.

I. Dueramae, A. Pengdam and S. Rimdusit (2012) [36] developed highly filled graphite based polybenzoxazine composites. Figure 3.2 shows the experimentally measured thermal conductivity of the composites with different graphite content at 25°C. The thermal conductivity increases with the increasing graphite contents. At 80% loading of graphite, thermal conductivity increases to 10.2 W/mK, more than 44 times that of pure polybenzoxazine (0.23 W/mK). This rapid growth may be attributed to the significant conductive pathways formed in the composite. As per the recent benchmark given by Department of Energy, USA the recommended value of thermal conductivity for bipolar plate is to be graphite than 10 W/mK. The highly filled graphite-polybenzoxazine composites at 80% loading of graphite content are a

promising bipolar plate for the fuel cell application as it shows relatively high thermal conductivity. The value is substantially greater than the DOE requirement.

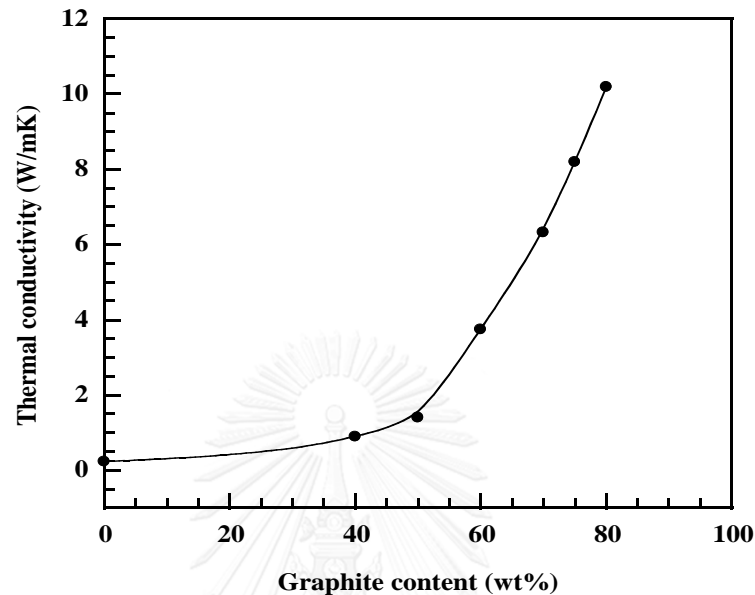


Figure 3.2 Thermal conductivity at 25°C of graphite filled polybenzoxazine as a function of filler contents.

I. Dueramae, A. Pengdam and S. Rimdusit (2012) [36] developed highly filled graphite based polybenzoxazine composites. Figure 3.3 shows electrical conductivity of the highly filled systems of graphite and polybenzoxazine composites at different content of graphite. From the result the electrical conductivity of the composites increased non-linearly when the graphite content increased up to 80% by weight. At 40-60% by weight of the graphite, the electrical conduction values increased only slightly with the filler loading. After 60% by weight of the graphite, the electrical conductivity values tended to increase sharply up to about 245 S/cm

The phenomenon is due to the gradual formation of the percolating network of the graphite particles within the plate with an increase in the graphite content. As per the recent benchmark given by Department of Energy, USA the recommended value of electrical conductivity for bipolar plate is to be graphite than 100 Scm^{-1} . The highly filled graphite-polybenzoxazine composites at 70 and 80% by weight of graphite content are a promising bipolar plate for the fuel cell application as it shows relatively high electrical conductivity of 104 and 245 S/cm, respectively. The value is substantially greater than the DOE requirement.

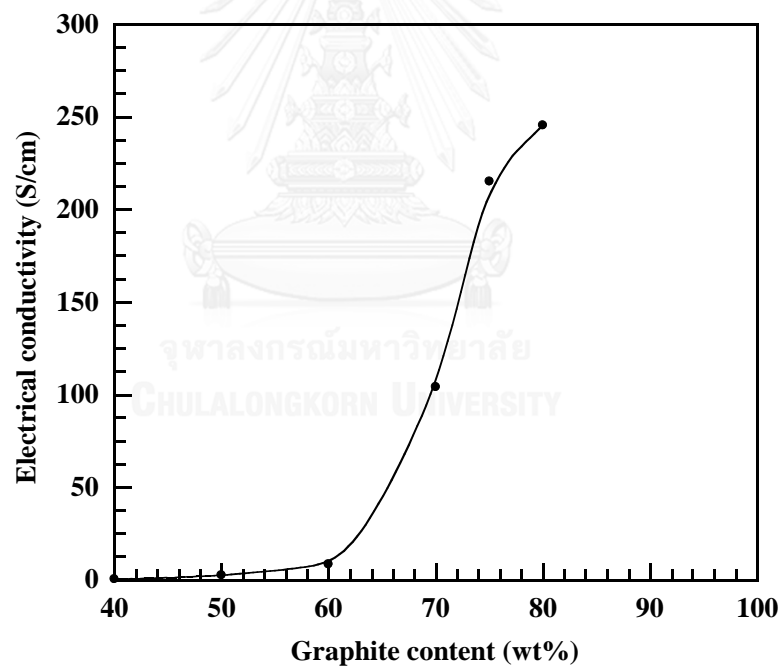


Figure 3.3 Effect of the graphite content on electrical conductivity (in-plane) of graphite filled polybenzoxazine composites.

R. Plengudomkit, M. Okahwilai and S. Rimdusit (2014) [37] developed highly filled graphene based polybenzoxazine composites. Figure 3.4 shows electrical conductivity of the highly filled of graphene and polybenzoxazine composites at different content of graphene. From the result, the electrical conductivity of graphene filled polybenzoxazine composites increased non-linearly when the graphene content increased up to 60% by weight. The electrical conduction values increased slightly at 10-30% by weight of the graphene filler. After 30% by weight of the graphene filler, the conductivity values tended to increase sharply up to about 357 S/cm. The phenomenon is due to the gradual formation of the percolating network of the graphene particles within the plate with an increase in the graphene content. Furthermore, electrical conductivity values of the graphene filled polybenzoxazine composites at 50 by weight (125 S/cm) and 60 by weight (357 S/cm) meet the value recommended by the US Department of Energy (DOE) of 100 S/cm.

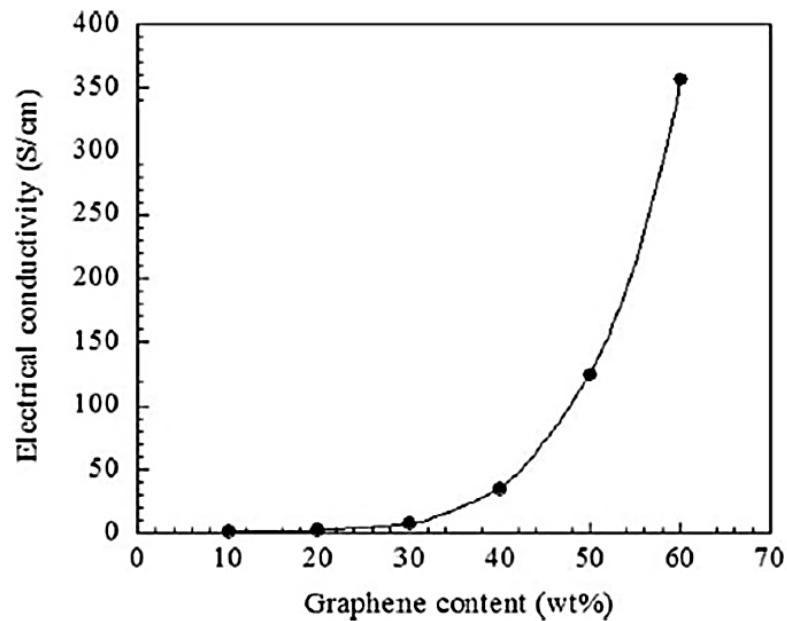


Figure 3.4 Effect of the graphene contents on electrical conductivity (in plane) of highly filled graphene-polybenzoxazine composites.

R. Plengudomkit, M. Okahwilai and S. Rimdusit (2014) [37] developed the flexural properties of highly filled graphene based polybenzoxazine composites. Figure 3.5 showed a plot of the flexural properties of graphene filled polybenzoxazine composites as a function of graphene contents. From the result the flexural modulus of composites increase with the increasing graphene contents. The flexural modulus values in a range of 5.2 to 17.5 GPa and highest values of 17.5 GPa at 60% by weight of graphene, which was enhanced by almost 246% compared to that of neat polybenzoxazine. The enhancement in flexural modulus was believed to be due to a uniform dispersion and strong interfacial bonding between the filler and the polybenzoxazine matrix.

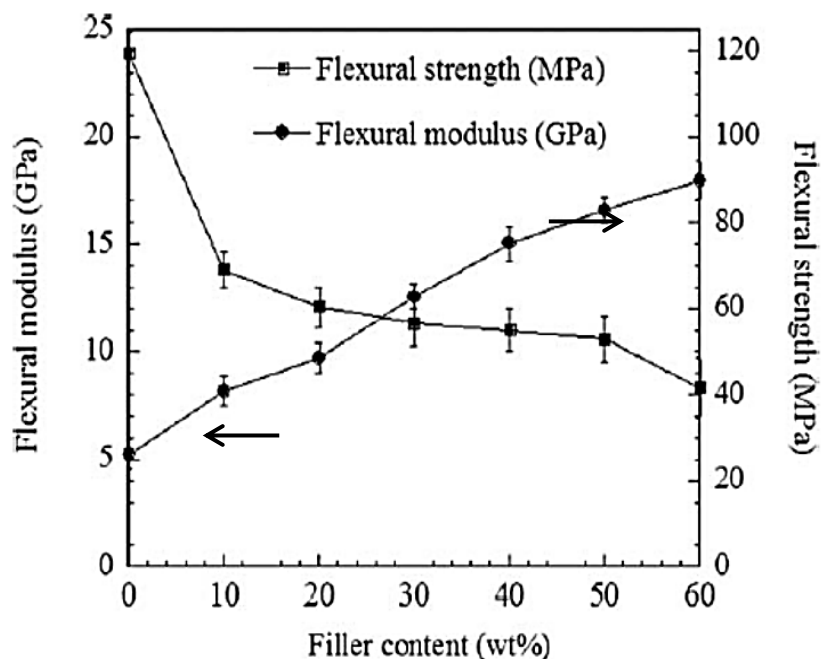


Figure 3.5 Relationship between graphene contents and the flexural properties of graphene-filled polybenzoxazine composites.

The flexural strength of composites decreases with the increasing graphene contents. The flexural strength values of composites lower than that of neat polybenzoxazine. At 10% by weight of graphene loading, the flexural strength of composites rapidly decrease from 119.7 of neat benzoxazine to 69.1 MPa. At 10-60% by weight of graphene loading, the flexural strength decreased slightly to 41.7 MPa. This behavior is due to the presence of interface between the filler and the matrix of these heterogeneous systems. Interestingly, the lowest flexural strength values of 41.7 MPa at 60% by weight of graphene was significantly greater than DOE targets of 25 MPa.

B. K. Kakati, A. Ghosh and A. Verma (2013) [38] developed electrical conductivity of composites from resole phenol formadehyde resin (resole-PF) as polymer matrix and natural graphite (NG), carbon black (CB), carbon fiber (CF) and graphene as filler. In research compared three composite systems. First, the composite were 70vol% of natural graphite and 5vol% of carbon black filled in 25vol% of matrix. Second, the composite were 65vol% of natural graphite, 5vol% of carbon fiber and 5vol% of carbon black filled in 25vol% of matrix. Third, the composite were 64vol% of natural graphite, 5vol% of carbon fiber, 5vol% of carbon black and 1vol% of graphene filled in 25vol% of matrix.

Table 3.1 Properties of composite bipolar plate

Properties	Contents (vol%)		
	NG 70%	NG 65%, CF 5%	NG 64%, CF 5%, GP 1%
Flexural strength (MPa)	45.9	54.2	57.2
In plane electrical conductivity (S/cm)	424.9	415.1	435.3
Through plane electrical conductivity (S/cm)	115.7	99.7	130.2

Table 3.1 show increase flexural strength when compared to that of previous optimum composition but the electrical conductivity decrease when filled carbon fiber in composite due to carbon fiber was non uniform dispersion in composite.

While, flexural strength and electrical conductivity increase when filled 1vol% of graphene filler in composite. From the result, it was found that at 1vol% of graphene loading increase the flexural strength of the composite from 54 to 57 MPa and in-plane electrical conductivity value of the composite from 415 to 435 S/cm.

A.Ghosh. P. Goswami. P. Mahanta and A. Verma (2014) [39] developed the flexural properties of carbon-polymer composite bipolar plate using novolac phenol formaldehyde resin (NPFR) as polymer matrix filled with natural graphite (NG), carbon black (CB), carbonfiber (CF) and graphene (GP). In this research fixed carbon fiber and carbon black at 5vol% and vary graphene content from 0-2.5vol% which added at the expanse of graphite. From figure 3.6 shows flexural strength of composite, the maximum flexural strength was 62.35 MPa at 1.5% by volume of graphene. From the result, the flexural strength of composite decreased very fast above 1.5% of graphene content. At 0-1.5% of graphene content, the flexural strength of composite was increased. Beyond 1.5% of graphene content was easily fractured due to improper owing to insufficient to significantly improve the mechanical properties of composite. Interestingly, the lowest flexural strength values of 39 MPa at 2.5% by volume of graphene was significantly greater than DOE targets of 25 MPa.

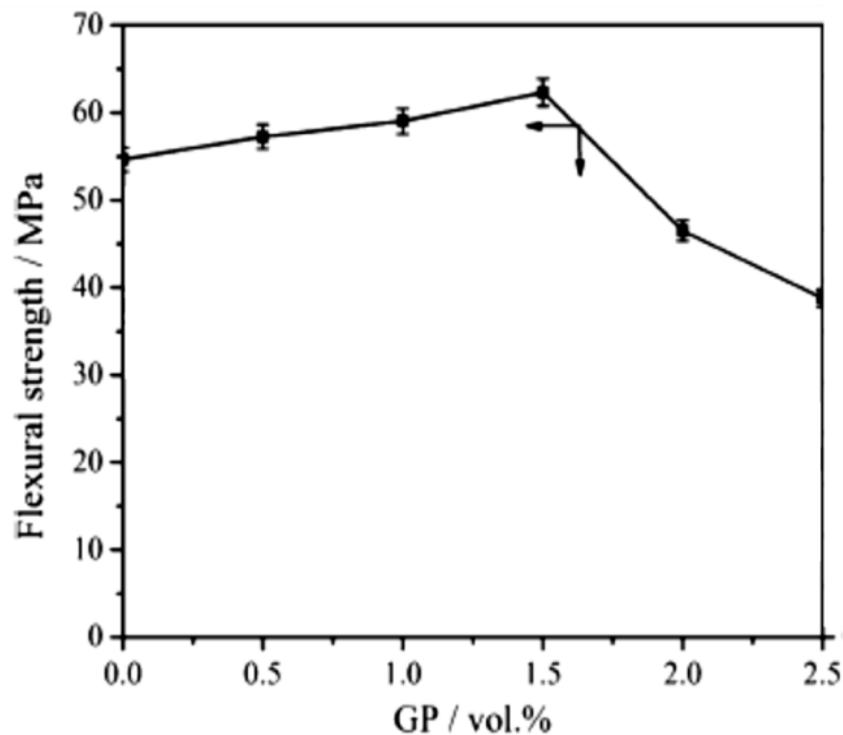


Figure 3.6 Effect of graphene content on flexural strength of developed composite bipolar plate (CF/CB/(NG+GP)/NPFR 5/5/60/30 vol%)

A.Ghosh. P. Goswami. P. Mahanta and A. Verma (2014) [39] developed the electrical and thermal conductivity of carbon-polymer composite bipolar plate using novolac phenol formadehyde resin (NPFR) as polymer matrix filled with natural graphite (NG), carbon black (CB), carbonfiber (CF) and graphene (GP). In this research fixed carbon fiber and carbon black at 5vol% and vary graphene content from 0-2.5vol% which was added at the expense of graphite. The electrical and thermal conductivity increased with increasing graphene content. The electrical conductivities, in-plane and through-plane, increase with the increasing graphene

content. The in-plane as well as through-plane electrical conductivities increase up to the graphene content of 1.5 % and beyond that it decreases. The pattern may be understood by the fact that the graphene has very high surface area as compared to graphite. As graphene was reinforced at the expense of graphite, more resin matrix was needed to coat the entire graphene surface to bind properly without any air/gas pocket especially above 1.5 % graphene content. The in-plane thermal conductivity of composite plates increased with increasing graphene content. The thermal conductivities of the bipolar plates were increased with the reinforcement of small amount of graphene content of the expense of graphite. Moreover, with the addition of 1.5 % graphene content, thermal conductivity increased around 40 %. However, it was found that beyond 1.5 %, the thermal conductivity was not improved. It may be due to the formation of air pockets in the composite owing to high requirement of matrix by graphene as compared to graphite, which hinder the thermal transport in the composite. It also supplemented the electrical conductivity results.

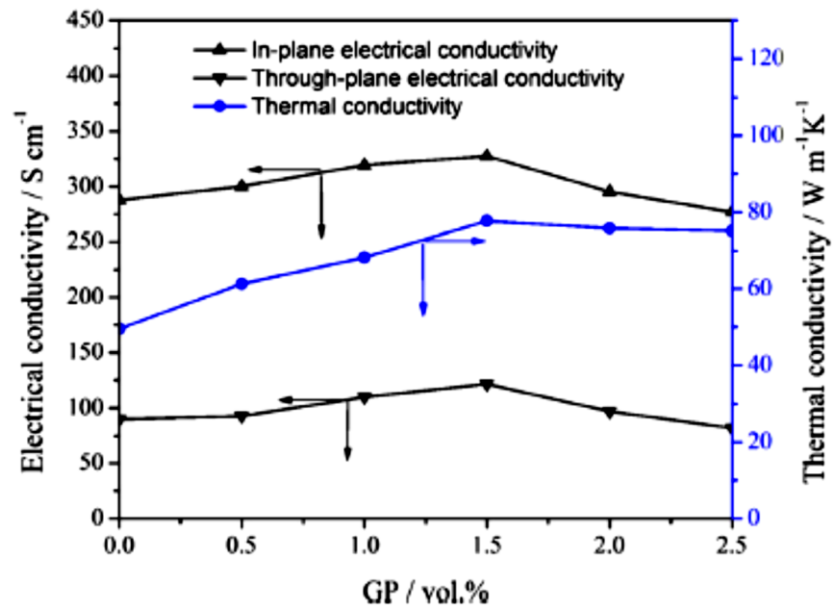


Figure 3.7 Effect of graphene content on in-plane, through-plane electrical conductivity and in-plane thermal conductivity of developed composite bipolar plate

(CF/CB/(NG+GP)/NPFR 5/5/60/30 %)

CHAPTER IV

EXPERIMENTAL

4.1 Materials and Monomer Preparation

The materials in this research are benzoxazine resin, graphite, graphene. Benzoxazine resin (BA-a) is based on bisphenol-A, aniline, and formaldehyde. Thai Polycarbonate Co., Ltd. (TPCC) supplied the bisphenol-A (polycarbonate grade). Paraformaldehyde (AR grade) was purchased from Merck Company and aniline (AR grade) was obtained from Panreac Quimica SA Company. Graphite (grade IG-70, density: 2 g/cm^3) was supplied by Toyo Tanso (Thailand) Co., Ltd. XGnP Graphene Nanoplatelets (Grade H) was purchased from XG Sciences, USA.

4.1.1 Benzoxazine Monomer Preparation

The benzoxazine resin used is based on aniline, bisphenol-A and paraformaldehyde in the molar ratio of 4:1:2. The reactant mixture was constantly stirred at 110°C for 40 min based on a solventless technology in the U.S. Patent 5,543,516. The obtained benzoxazine monomer is light yellow solid at room temperature and can be molten to yield a low viscosity resin at temperature in the range of $70\text{-}80^\circ\text{C}$. The product is then ground to fine powder and can be kept in a refrigerator for future-use. The density is 1.2 g/cm^3 .

4.1.2 Graphite Characteristics

Graphite grade IG-70 was supplied by Toyo Tanso (Thailand) Co., Ltd. The density is 2.0 g/cm^3 . It has a reported Young's modulus is 11.8 GPa, electrical resistivity is $10 \mu\Omega\cdot\text{m}$ and coefficient thermal expansion is $4.6 \times 10^{-6} / \text{K}$.

4.1.3 Graphene Characteristics

XGnP Graphene Nanoplatelets grade H was purchased from XG Sciences USA. (purity 99.5%). The diameter and thickness of grade H Graphene Nanoplatelets is 5 to $25 \mu\text{m}$ and 15 nm thick with surface area of $50\text{-}80 \text{ m}^2 / \text{g}$. The density is 2.2 g/cm^3 .

4.2 Specimen Preparation

The graphite average aggregate sizes (<50, 140 and $240 \mu\text{m}$) filled polybenzoxazine were prepared with graphite loadings of 70, 75, 80 and 85% by weight to yield molding compounds. The graphite/graphene filled polybenzoxazine composites were prepared by varying composition of graphite and graphene. The graphite aggregate size of $240 \mu\text{m}$ was used for all samples. The overall carbon filler content was fixed at 83wt% and varying composition of graphene from 0-10wt% at an expense of the graphite. The graphite and graphene was firstly dried at 100°C for 24 hours in an air-circulated oven until a constant weight was achieved and was then kept in a desiccator at room temperature. The filler was mechanically stirred to achieve uniform dispersion in benzoxazine resin using an internal mixer at about 110°C for 40 minute. The compound was compression-molded by hot pressing for

thermal-cured specimen. The hot-press temperature of 150°C was applied for 1 hour and 200°C for 3 hours using a hydraulic pressure of 15 MPa. The thickness was controlled by using a metal spacer. All samples were air-cooled to room temperature in the open mold and were cut into desired shapes before testing.

4.3 Characterization Methods

4.3.1 Differential Scanning Calorimetry (DSC)

Curing characteristics of the graphite/graphene filled polybenzoxazine composites were examined by a differential scanning calorimeter model DSC1 Module from Mettler-Toledo (Thailand). For each test, a small amount of the sample ranging from 5 to 10 mg was placed in an aluminum pan and sealed hermetically with an aluminum lid. The experiments were performed in a temperature range of 30°C up to 300°C. The purge nitrogen gas flow rate was maintained to be constant at 50 ml/min and a heating rate of 10°C /min. The processing temperature, time and glass transition temperature were obtained from the thermograms while the percentage of resin conversion was calculated from the DSC thermograms.

4.3.2 Density Measurement

Actual Density Measurement

The density of each specimen was determined by water displacement method according to ASTM D 792 (Method A). All specimens were prepared in a

rectangular shape with 50 mm in length, 25 mm in width and 2 mm in thickness. Each specimen was weighed in air and in water at $23 \pm 2^\circ\text{C}$. The density was calculated using Equation (4.1). An average value from at least five specimens was calculated.

$$\rho = \frac{A}{A-B} \times \rho_0 \quad (4.1)$$

where

- ρ = Density of the specimen (g/cm^3)
- A = Weight of the specimen in air (g)
- B = Weight of the specimen in liquid (water) at $23 \pm 2^\circ\text{C}$ (g)
- ρ_0 = Density of the liquid (water) at the given temperature (g/cm^3)

Theoretical Density Measurement

The theoretical density by mass of polybenzoxazine filled with graphite/graphene can be calculated as follow:

$$\rho_c = \frac{1}{\frac{W_f}{\rho_f} + \frac{(1-W_f)}{\rho_m}} \quad (4.2)$$

Where ρ_c = Composite density, g/cm^3

ρ_f = Filler density, g/cm^3

ρ_m = Matrix density, g/cm³

W_f = Filler weight fraction

$(1-W_f)$ = Matrix weight fraction

4.3.3 Dynamic Mechanical Analysis (DMA)

Dynamic mechanical property was measured with dynamic mechanical analyzer (DMA) model DMA242 from NETZSCH Instrument. The dimension of specimens was with 50 mm in length, 10 mm in width and 2.5 mm in thickness. The test was performed under the three-point bending mode. A strain in the range of 0 to 30 μm was applied sinusoidally at a frequency of 1 Hz. The temperature was scanned from 30°C to 300°C and a heating rate of 5°C/min. The purge nitrogen gas flow rate was maintained to be constant at 50 ml/min. The glass transition temperature was taken as the maximum point on the loss modulus curve in the temperature sweep tests. The storage modulus (G') and loss modulus (G'') were then obtained. The glass transition temperature (T_g) was taken as the maximum point on the loss modulus curve in the DMA thermograms.

4.3.4 Thermogravimetric Analysis (TGA)

The thermal stability of graphite/graphene filled polybenzoxazine composites were measured using a thermogravimetric analyzer model TGA1 Module from Mettler-Toledo (Thailand). The initial mass of the composite to be tested was about

10 mg. It was heated from 25°C to 1000°C for all composites at a heating rate of 20°C/min under nitrogen atmosphere. The degradation temperature at 5% weight loss and solid residue of each specimen determined at 800°C were recorded for each specimen.

4.3.5 Specific Heat Capacity Measurement

Specific heat capacities of all samples were examined by a modulating differential scanning calorimeter (MDSC) model DSC1 Module from Mettler-Toledo (Thailand). All samples were crimped in non-hermetic aluminum pans with lids. The weight of sample is in the range of 15 to 20 mg. The sample was purged with dry nitrogen gas at a flow rate of 60 ml/min. The temperature was scanned from 15°C to 200°C at a heating rate of 1°C /min.

4.3.6 Thermal Diffusion Measurement

Thermal diffusivity of the graphite/graphene-filled polybenzoxazine composites were measured by laser flash diffusivity instrument (Nano-Flash-Apparatus, LFA 447, NETZSCH). The composite specimens were prepared in a square shape with 10 mm in length, 10 mm in width and 1 mm in thickness. All measurements were conducted at atmosphere from room temperature to 180°C. The specimens were subjected to a short duration thermal pulse by laser. The energy of the pulse absorbed at the front face results in the temperature rise in the rear face. The temperature rise was hem collected by a collecting system. Thermal

diffusivity (α) was calculated from the half-rise constant ($k= 0.13879$ under ideal conditions at half-rise), the specimen thickness (L) and the time ($t_{1/2}$) for the rear face temperature to reach half of its maximum value and thermal diffusion was calculated from Equation 4.3. For each specimen, its thermal diffusivity was averaged from three measurements at each temperature.

$$\alpha = \frac{kL^2}{t_{0.5}} \quad (4.3)$$

4.3.7 Thermal Conductivity Measurement

The through-plane thermal conductivity (k) was calculated using the measured density (ρ), specific heat capacity at constant pressure (C_p), and the measured thermal diffusivity (α) of all sample obtained through Equation 4.4.

$$k = \rho \times C_p \times \alpha \quad (4.4)$$

4.3.8 Flexural Properties Measurement

A Universal Testing Machine (model 5567) from Instron Instrument was used to study flexural properties of the graphite/graphene filled polybenzoxazine composite specimens. The dimensions of the composite specimens were prepared with 50 mm in length, 25 mm in width and 2 mm in thickness. The test method used is a three-point bending mode with a support span of 32 mm. Bending test was performed at the crosshead speed of 0.85 mm/min. The flexural modulus and the

flexural strength of each composite were determined according to the procedure set out in ASTM D 790M, they were calculated by Equations 4.5 and Equations 4.6.

$$E_B = \frac{L^3 m}{4bd^3} \quad (4.5)$$

$$S = \frac{3PL}{4bd^2} \quad (4.6)$$

Where

- E_B = Flexural modulus, MPa
- S = Flexural strength, MPa
- P = Load at a given point on the load-deflection curve, N
- L = Support span, mm
- b = Width of the beam tested, mm
- d = Depth of the beam tested, mm
- m = Slope of the tangent to the initial straight-line portion of the load deflection curve, N/mm.

4.3.9 Water Absorption

Water absorption measurements were conducted following ASTM D570 using disk-shaped specimens having a 50 mm diameter and a 3 mm thickness. All specimens were conditioned, weighed, and submerged in distilled water at 25°C. The specimens were occasionally removed, wiped dry, weighed, and immediately

returned to the water bath. The amount of water absorbed was calculated based on the initial conditioned mass of each specimen.

4.3.10 Electrical Conductivity Measurement

The in-plane electrical conductivity of graphite/graphene filled polybenzoxazine composites was measured by a mirror galvanometer with a universal shunt and an HP 4284A impedance analyzer. The HP 4284A programmable current source was used for providing constant voltage drop (V) while current (I) supply in between two pinpoints was measured by HP 4284A auto ranging ampere. The dimension of a round shape specimen was 100 mm in diameter and 2.0 mm in thickness. An average electrical conductivity value from of about 4-5 readings on each plate (in plane) was reported.

4.3.11 Scanning Electron Microscope (SEM)

Interfacial bonding of a filled sample was investigated using a JSM-6400 scanning electron microscope (SEM) at an acceleration voltage of 15 kV. All specimens were coated with thin film of gold using a JEOL ion sputtering device (model JFC-1200) for 4 min to obtain a thickness of approximately 30Å and the micrographs of the specimen fracture surface were taken. The obtained micrographs were used to qualitatively evaluate the interfacial interaction between the graphite/graphene filler and the matrix resin.

CHAPTER V

RESULTS AND DISCUSSION

5.1 Graphite-filled Polybenzoxazine Characterization

5.1.1 Actual Density and Theoretical Density Determination of Graphite Filled Polybenzoxazine Composites

Density of composites is a key parameter used to efficiently evaluate the quality of composites due to the void formation or air gap in the samples. Figure 5.1 exhibits the density of graphite filled polybenzoxazine composites as a function of filler content. The theoretical densities of the composites were calculated based on the density of graphite of 2.0 g/cm^3 and the density of polybenzoxazine of 1.19 g/cm^3 [8]. From the results, the theoretical and actual densities of the graphite filled polybenzoxazine composites were linearly increased with increasing graphite content following the rule of mixture thus suggesting negligible void or air gap in the composites samples. In this study, the maximum packing density of three sizes of graphite (<50, 140 and 240 μm) was determined at the point that the observed density is equal to their theoretical density. The maximum packing densities of three sizes of graphite are summarized in Table 5.1. The maximum packing densities of different graphite sizes at <50, 140 and 240 μm were 75wt%, 80wt% and 83wt%, respectively. The highest maximum packing density was 74vol% or about 83wt% of graphite size 240 μm . The attempt to add graphite beyond 83% by weight, the

observed composite packing density tended to decrease to a value lower than the theoretical value due to void formation. From the experiment, the larger aggregate size of graphite in the composite showed higher the maximum packing density of the composite rendered high thermal and electrical conductivity due to the capability of forming conductive networks with low resistance, which is in good agreement with the theory of particle packing. the packing density decreases with smaller particle size due to an increase in particle surface area, lower particle mass, and a greater importance of weak short-range forces including electrostatic fields and surface adsorption of moisture and other wetting liquids that can lead to agglomeration [8]. As a consequence, the use of graphite at size of 240 μm having large average particle size should be sufficient in obtaining high particle packing [8].

5.2 Graphite/Graphene Filled Polybenzoxazine Characterization

5.2.1 Curing Behavior of Graphite/Graphene Filled Polybenzoxazine Composites with Curing Condition

The curing reaction of benzoxazine resin filled with graphite/graphene fillers observed by differential scanning calorimeter in a temperature range of 30°C to 300°C and a heating rate of 10°C/min. The overall carbon filler content was fixed at 83wt% and varying composition of graphene from 0-10wt% at an expense of the graphite. Figure 5.2 shows curing exotherm of the neat benzoxazine resin (BA-a) and benzoxazine resin filled with graphite/graphene molding compounds at different carbon filler content. The exothermic peak of the neat benzoxazine resin centered at

233°C was attributed to the ring-opening polymerization of its oxazine-ring. The characteristic exothermic peak of 0, 2.5, 5, 7.5 and 10wt% of graphene content in benzoxazine molding compound were 232, 220, 212, 204 and 202°C, respectively. The unchanged exothermic peak position of the 83wt% graphite loading (0wt% graphene loading) compared to the neat benzoxazine resin indicated that graphite has negligible effect on curing reaction of the benzoxazine monomers as shown in Figure 5.3. Interestingly, exothermic peak position of benzoxazine molding compounds shifted to lower temperature with higher amount of graphene loading indicating that graphene can act as a catalyst for ring-opening polymerization of its oxazine-ring thus minimized the curing condition in terms of energy consumption to undergo polymerization.

The result of the catalytic reaction was also confirmed by FTIR spectra of pure graphene as can be seen in Figure 5.4. The characteristic peak of the carboxylic (COOH) group was noticed at 1733 and 3444 of C=O stretching and O-H stretching, respectively. These noticeable peaks were also observed by K. J. Huang [40]. The effect of carboxylic group on the catalyst of ring-opening polymerization of polybenzoxazine was also noticed by P. Kasemsiri in the study of cashew nut shell liquid and benzoxazine resin [41].

Moreover, area under exothermic peak indicated the heat of reaction of the polymerization process. As shown in Figure 5.2, the area under the exothermic peaks

decreased with increasing the graphene content in the molding compounds. The values reduced from 335 J/g of the neat benzoxazine resin to 30 J/g of molding compound containing 10wt% of graphene (73wt% of graphite loading). The area was reduced because of the partially cure of benzoxazine resin increases with increasing graphene content when mixing by an internal mixer at temperature of 110°C for 40 minute and a mixing speed of 40 round per minute.

Figure 5.5 shows the DSC thermograms of graphite/graphene filled benzoxazine molding compound at 2.5wt% of graphene loading (80.5wt% of graphite loading) cured by conventional thermal method at 200°C at various curing times. At temperature of 200°C, polymerization by ring-opening reaction of the benzoxazine monomer could proceed at a relatively fast rate and provided good cured specimens. From the results, the uncured benzoxazine molding compound possessed a heat of reaction determined from the area under the exothermic peak to be 252 J/g and the value decreased to 23, 11 and 4 J/g, after curing at 200°C for 1 hour, 2 hours and 3 hours, respectively. The degree of conversion calculated by Equation 5.1 was 98% after curing at 200°C for 3 hours. Therefore, the curing condition at 200°C for 3 hours was used to cure all benzoxazine molding compounds to prepare the specimens for further characterization.

$$\% \text{ conversion} = 1 - \frac{H_{\text{rxn}}}{H_0} \times 100 \quad (5.1)$$

where: H_{rxn} is the heat of reaction of the partially cured specimens.

H_0 is the heat of reaction of the uncured resin.

5.2.2 Dynamic Mechanical Properties of Graphite/Graphene Filled Polybenzoxazine Composites

The dynamic mechanical analysis plots of the storage modulus (E') of the graphite/graphene filled polybenzoxazine composites versus the graphene content ranging from 0 to 10wt% are shown in Figure 5.6. As seen from the results of storage modulus at 35°C in Figure 5.6, the graphite/graphene filled polybenzoxazine composites tended to increase with increasing graphene content. The storage modulus at 35°C of the neat polybenzoxazine was 5.9 GPa. These values were consistent with the results reported by R. Plengudomkit et al [37]. The storage modulus of the composites were ranging from 12.2 GPa to 16.9 GPa of the composites with 0-10wt% of graphene contents. The maximum storage modulus value of 7.5wt% of graphene increased 11 GPa or about 186% enhancement compared to the neat polybenzoxazine. This phenomenon is likely due to the reinforcing effect of the graphene in graphite/graphene filled polybenzoxazine composites. The results also suggested the substantial interfacial adhesion between the filler and the polybenzoxazine matrix. Furthermore, the moduli of the graphite/graphene filled polybenzoxazine in the rubbery plateau region were also

investigated and were found to increase with increasing amount of the graphene implying substantial interaction between the filler and the polymer matrix.

Loss modulus curves of graphite/graphene filled polybenzoxazine at 0-10wt% of graphene contents as a function of temperature were investigated as shown in Figure 5.7 and the glass-transition temperatures (T_g) obtained from the maximum peak of loss modulus of the graphite/graphene filled polybenzoxazine composites were also reported. The T_g values of the composites were observed to be in the range of 200 to 209 °C with 0-10wt% of graphene contents which were higher than the T_g of the neat polybenzoxazine as reported to be 174°C [37]. The maximum T_g was 209°C at 10wt% of graphene which was 35°C higher than the neat polybenzoxazine. In addition, it could be seen that the T_g values slightly increased with increasing graphene contents in the polybenzoxazine composites. This phenomenon also implies good adhesion between the graphene filler and the polybenzoxazine matrix and flake-like shape of graphene filler which substantially impedes the polymeric chain movement reflecting in the observed higher T_g values [36, 42].

5.2.3 Effect of Graphene Loading on Thermal Stability of Graphite/Graphene Filled Polybenzoxazine Composites

Thermal stability of the graphite/graphene filled polybenzoxazine composites was investigated by TGA under a nitrogen atmosphere. One common parameter used to determine temperature stability of polymeric composites is degradation temperature (T_d). The TGA curves of neat polybenzoxazine, graphite, graphene and graphite/graphene filled polybenzoxazine composites with different graphene loadings are shown in Figure 5.8. In Figure 5.8, the polybenzoxazine matrix showed of 320°C at its 5% weight loss and the char residue of 25% at 800°C. These values were consistent with the results reported by S. Rimdusit et al. [36, 43]. The pure graphite shows outstandingly high thermal stability whereas the pure graphene showed T_d of 463°C was obtained at a 5% weight loss and char residue of 91% at 800°C. The weight loss of pure graphene in range of 200 to 700 °C might be associated with the removal of oxygen-containing functional groups such as carboxyls, or hydroxyls [40], which were reported to be naturally presented during typical graphene synthesis such as that suggested in the technical data sheet of graphene nanoplatelets-grade H from XG Sciences, USA [44]. In addition, the carboxyls functional group was also confirmed by FTIR spectra of the pure graphene as it can be seen in Figure 5.4. The presence of oxygen-containing functional groups in graphene has been reported to help improve the modulus of the composites from better interfacial bonding with the matrix [45].

As can be seen in Figure 5.8, the T_d at 5% weight loss of our graphite/graphene filled polybenzoxazine composites with 0 to 10wt% of graphene loading were found to slightly increase with increasing graphene contents. The T_d values of the composites were reported to be in the range of 425 to 433°C. The maximum T_d value of the composite at 10wt% of graphene content was 433°C, enhanced by 113°C compared to that of the unfilled polybenzoxazine. This enhancement is attributed to the graphene flakes which acted as a gas barrier and could delay the decomposition of volatile products [42, 46].

Char residue of the graphite/graphene filled polybenzoxazine composites were illustrated in Figure 5.9. Char content of the composites was found to not change with increasing graphene contents. In principle, the higher char residue can provide a sample with enhanced flammability [47].

5.2.4 Specific Heat Capacity of Graphite/Graphene Filled Polybenzoxazine Composites at Various Graphene Contents

Specific heat capacity of composite materials is an essential parameter especially in the determination of thermal conductivity because it relates thermal diffusivity and thermal conductivity [48]. The specific heat of a material is defined as the amount of heat per unit mass required to raise the temperature by one degree Celsius. Figure 5.10 exhibits specific heat capacity at 25°C of graphite/graphene filled polybenzoxazine composites at different graphene loading ranging from 0 to 10wt%.

From this figure, the specific heat capacity of the composites was found to increase with increasing graphene loading. This phenomenon was expected from the higher specific heat capacity of the graphene compared to the graphite. Moreover, the specific heat capacity of the composites is the structure-insensitive property characteristic, which having a linear relationship with the weight of filler [48].

Most specific heat capacity values of composites at different filler loading are normally obtained by using the rule of mixture when the heat capacities of the filler (graphite and graphene) and the matrix are known [48]. Specific heat capacity for three phase system according to rule of mixture is shown in Equation 5.2

$$C_{pc} = C_{p,\text{graphite}}W_{\text{graphite}} + C_{p,\text{graphene}}W_{\text{graphene}} + C_{pp}(1-W_f) \quad (5.2)$$

where C_{pc} and C_{pp} are the specific heat capacities of the composite and polymer, respectively, W_f is the mass fraction of the filler.

From our measurement, the specific heat capacity of the pure graphite, pure graphene and the neat polybenzoxazine were reported to be 0.770, 1.075 and 1.756 J/gK, respectively. Therefore, specific heat capacity values at different filler loading are normally predicted by the rule of mixture according to Equation 5.2. The values were then substituted in Equation 5.2, and the corresponding equation then became:

$$C_{pc} = 0.770W_{\text{graphite}} + 1.075W_{\text{graphene}} + 1.756(1-W_f) \quad (5.3)$$

The specific heat capacity values of the polybenzoxazine composites with different filler contents obtained from the experimental results were compared with the values calculated from Equation 5.3. The specific heat capacity values of different filler contents from the experimental results are thus in good agreement with those predicted by the rule of mixture as seen in Table 5.3. The specific heat capacity of composites is an important parameter for the determination of thermal conductivity. In theory, thermal conductivity can be determined from the known thermal diffusivity, density and heat capacity values using Equation 4.4.

5.2.5 Effects of Graphene Contents on Thermal Diffusivity of Graphite/Graphene Filled Polybenzoxazine Composites

Thermal diffusivity is the thermal conductivity divided by density and specific heat capacity at constant pressure. It measures the ability of a material to conduct thermal energy relative to its ability to store thermal energy [49]. Thermal diffusivity measurements are generally conducted with the “laser flash” technique, which being a relatively fast and accurate method and using a small sample. The thermal diffusivity of graphite/graphene filled polybenzoxazine as a function of graphene loadings was measured at 25°C as shown in Figure 5.11. From Figure 5.11, thermal diffusivity of graphite/graphene filled polybenzoxazine composites tended to increase with increasing graphene content due to the presence of highly thermally conductive graphene.

Furthermore, the thermal diffusivities of graphite/graphene filled polybenzoxazine composites as a function of temperature are shown in Figure 5.12. From the figure, it was observed that thermal diffusivity values of the samples decreased with increasing temperature due to more pronounced phonon-phonon scattering or heat resistant phenomena in the samples [50]. Moreover, the composites with a higher graphene loading (lower graphite loading) showed a higher slope in its thermal diffusivity value with temperature than those with a lower filler content suggesting a more temperature sensitivity of the composites with increasing the graphene contents.

5.2.6 Thermal Conductivity of Graphite/Graphene Filled Polybenzoxazine Composites

The bipolar plate must be thermally conductive to conduct the generated heat from an active area of the fuel cell to a cooling channel, to control the stack temperature and to achieve a homogeneous temperature distribution in each cell and over the whole active area, therefore; thermal conductivity is a critical bipolar plate characteristic. Thermal conductivity refers to the amount/speed of heat transmitted through a material. Heat transfer occurs at a higher rate across materials of high thermal conductivity than those of low thermal conductivity. Thermal conductivities of the graphite/graphene filled polybenzoxazine composites as a function of graphene loading at 25°C were calculated according to Equation 4.4 with

the known parameters of thermal diffusivities, heat capacities and densities of the composites. The values were also summarized in Table 5.6.

Figure 5.13 shows the thermal conductivity of graphite/graphene filled polybenzoxazine composites as a function of graphene loading. The thermal conductivity of the neat polybenzoxazine was calculated to be 0.23 W/mK which is in good agreement with the previous reported value [36]. Moreover, the thermal conductivity values of the composites tended to slightly increase with increasing graphene content. At 0 to 7.5wt% of graphene loading, the thermal conductivity values of composites increase from 12.6 W/mK to 14.5 W/mK whereas the value at 10wt% of graphene was not improve by graphene loading. It may be the fact that the graphene has very high surface area as compared to graphite. As graphene was reinforced at the expense of graphite, more resin matrix was needed to coat the entire graphene surface to bind properly without any air/gas pocket especially at 10wt% of graphene content. The maximum thermal conductivity of graphite/graphene filled polybenzoxazine composites was determined to be 14.5 W/mK at 7.5wt% of the graphene which represented about 63 times greater than that of the neat polybenzoxazine. As a consequence, an incorporation of filler in graphite/graphene polybenzoxazine composites can provide a greater thermal conductivity compared to the composite with only graphite filler. In theory, graphite microfillers, owing to their relatively large size, should be beneficial in producing a

small number of interfaces, thus contributing to a high thermal conductivity in overall. In addition, adding a small amount of graphene nanofillers should enhance the interaction between the microfillers (by bridging the gaps between them) and increasing in contact area between microfillers due to the presence of nanofillers between them. This will further increase the thermal conductivity of the composite. The increased contact area can definitely lead to reduced contact resistance at the interface between the fillers and hence lead to higher thermal conductivities for the composites [51]. However, thermal conductivity values observed in our graphite/graphene filled composites were through-plane thermal conductivity which graphite and graphene are oriented in the pressure planes during composite manufacturing by compression molding. Through-plane thermal conductivity is commonly lower than in-plane value because of anisotropic structure of the filler, reported by X. Tian et al. [52].

Comparing at the maximum filler content, the thermal conductivity of our graphite/graphene filled polybenzoxazine composites was found to be 14.5 W/mK which greater than the values obtained from graphite filled polybenzoxazine which reported to be 10.2 W/mK by I. Dueramae et al. [36] and graphene filled polybenzoxazine composites which reported to be 8.03 W/mK by R. Plengudomkit et al. [37]. Furthermore, our highly filled graphite/graphene filled polybenzoxazine

composites also showed higher thermal conductivity value than some reported high filler loading composites.

5.2.7 Effect of the Graphene Loading on Flexural Properties of Graphite/Graphene Filled Polybenzoxazine Composites

One common function of bipolar plate is to provide mechanical strength and rigidity to support the thin membrane and electrodes and clamping forces for the stack assembly [11]. The flexural properties of graphite/graphene filled polybenzoxazine composites with different graphene loading were investigated. Flexural modulus of the neat polybenzoxazine and graphite/graphene filled polybenzoxazine composites are illustrated as a function of graphene content in Figures 5.14. The flexural modulus of the neat polybenzoxazine was 5.3 GPa. As displayed in Figure 5.14, the flexural modulus of the composites tended to increase with increasing graphene contents, following an additive rule. At 0 to 7.5wt% of graphene loading, the flexural modulus of composites increased from 12.4 GPa to 16.8 GPa whereas at 10wt% of graphene, the flexural modulus was 16.2 GPa which was lower than the others. It can be understood by the fact that the graphene has very high surface area as compared to graphite. At 10wt% of graphene content, more benzoxazine resin was needed to coat the entire graphene surface to bind properly without any air gap. Benzoxazine resin contents were fixed in all samples so the resin was not enough to coat the entire graphene surface then density of the composite was lower than theoretical density. The maximum flexural modulus of

graphite/graphene filled polybenzoxazine composite was 16.8 GPa at 7.5wt% graphene loading which represented about 140% greater than that of the pure graphite was to be 12 GPa. The phenomenon was due to a uniform dispersion and strong interfacial bonding between the carbon filler and the polybenzoxazine matrix [53]. In addition, graphene has more rigidity of particulate into the polybenzoxazine matrix attributed to significant enhancement in the stiffness of the obtained polybenzoxazine composites [36]. However, the flexural modulus of all graphite/graphene filled polybenzoxazine composites exceeded the DOE requirement of 10 GPa for a bipolar plate application [4, 18].

Figure 5.15 exhibits flexural strength of graphite/graphene filled polybenzoxazine composites. The flexural strength of the pure graphite was 47 MPa. The flexural strength of our composites tended to slightly decrease with increasing graphene content. For the composite at 0-10wt% of graphene loading, the strength of the composite decreased from 59 to 54 MPa. The flexural strength values of the composites were found to be higher than that of the pure graphite. This behavior is due to the increasing of interface between the filler and the matrix of these heterogeneous systems. Moreover, the graphene and graphite are platelet shape with almost the same dimensions in the planar direction so they do not act as reinforcing materials and cause a decrease in the effective cross-section area [54, 55]. In addition, at 10wt% graphene loading (73wt% of graphite loading), the flexural strength of our highly filled composite remains as high as 54 MPa, which was

significantly greater than the flexural strength value of the DOE targets for bipolar plate material (>25MPa) [4].

5.2.8 Water Absorption of Polybenzoxazine and Graphite/Graphene Filled Polybenzoxazine Composites at Various Graphene Contents

The mechanism of water absorption of the composites was studied from the amount of water absorption by the specimens. The water absorption was calculated from Equation 5.4

$$\text{Water absorption (\%)} = \frac{W - W_d}{W_d} \times 100 \quad (5.4)$$

where W is the weight of the specimen at time t , and W_d is the weight of the dry specimen [56].

Figure 5.16 shows water absorption behavior of the neat polybenzoxazine and its composites filled with graphite/graphene at different carbon filler content ranging from 0-10wt% of graphene or 73-83wt% of graphite up to 168 hours. From the figure, the percentage of water absorbed plotted versus time for all composites showed a similar behavior. The water absorption of specimens found to be more speedy increased during first stages (0-24 hours). The water uptake of typical composites for bipolar plate in fuel cell applications at 24 hours has to be less than 0.3%, which is the value required by Department of Energy (DOE) [57]. In experiment, our polybenzoxazine composites showed water uptake value at 24 hours was less

than 0.04% which was lower than required of Department of Energy (DOE). In addition, the water absorption of all composites was decreased with increasing graphene content. This phenomenon was attributed to the presence of the hydrophobic and water repelling nature of graphene surface that tended to immobilize some of moisture, which inhibited the water permeation in the polymer matrix [46, 58]. Moreover, graphene has plate-like shape filler with high aspect ratio provided indirect pathways for water molecules to enter the composites and could acted as efficient barriers against transport of water through the composites [46, 59]. In addition, good interfacial bonding between the filler and the matrix as well as excellent wetting of benzoxazine resin might also support to the substantial reduction of the water absorption values. This low water uptake is highly desirable characteristic in bipolar plate application.

5.2.9 Electrical Conductivity of Graphite/Graphene Filled Polybenzoxazine at Various Graphene Contents

According to function of bipolar plates in PEMFC, the bipolar plate must conducting electrons to complete the circuit. In order to fulfill aforementioned function, electrons must transfer from the anode to cathode through bipolar plates to complete a circuit, so one critical fuel cell performance factor is the electrical conductivity of the bipolar plate to minimize voltage loss. [60, 61]. In fuel cell bipolar plates, the in-plane conductivity is more important because the bipolar plate is thin in the through-thickness direction and the area is large in the in-plane direction.

Therefore, the in-plane electrical conductivity was tested in our experiment [2]. Figure 5.17 shows a plot of the in-plane electrical conductivity of graphite/graphene filled polybenzoxazine composites as a function of graphene loading. As can be seen in this figure, the electrical conductivity of the composites at 0-10wt% of graphene contents slightly increased with increasing graphene loading. The electrical conductivity of our composites at 0-10wt% of graphene contents increased from 284 S/cm to 329 S/cm. As a consequence, an incorporation of graphene in graphite/graphene polybenzoxazine composites can provide a greater electrical conductivity compared to the composite with only graphite filler. In theory, graphite microfillers, owing to their relatively large size, should be beneficial in producing a small number of interfaces, thus contributing to a high electrical conductivity in overall [51]. In contrast, the smaller particle composite system is likely to have the larger contact points and thus the contact resistance becomes larger because the contact points are insulated with the polymer matrix [2]. In addition, adding a small amount of graphene nanofillers help to make conducting tunnels between the graphite particles, and thus increase the electrical conductivity as similarly reported of graphite/carbon black filled epoxy system by [55].

In 2015, Department of Energy, USA the recommended value of electrical conductivity for bipolar plate more than 100 Scm^{-1} [4]. Our highly filled graphite/graphite filled polybenzoxazine composites at 0-10 wt% of graphene

content are a promising as bipolar plate for the fuel cell application as it shows relatively high electrical conductivity. The value is substantially greater than the DOE requirement.

5.2.10 SEM Characterization of Graphite/Graphene-Polybenzoxazine

The significant improvement in mechanical properties of the composites with incorporation of graphite/graphene fillers were further supported by SEM micrographs. Figure 5.18(a) to 5.18(e) shows the interfacial characteristics along the fracture surface of the pure graphite, pure graphene, neat polybenzoxazine and the graphite/graphene filled polybenzoxazine. Figure 5.18(a) shows the fracture surface of the neat polybenzoxazine revealing a relatively smooth surface. Figure 5.18(b) shows a SEM micrograph of the graphite aggregate at size 240 μm , platelets are flake-like shaped, and they consist of stacks of thin plates. From Figure 5.18(c) shows a SEM micrograph of graphene nanoplatelets, platelets are thin flake-like shaped. Figure 5.18(d) and Figures 5.18(e) shows a SEM micrograph of fracture surface of polybenzoxazine composites with 0.5wt%/0.5wt% of graphite/graphene filler and 80.5wt%/2.5wt% of graphite/graphene, respectively. As seen in the figure, the fillers were well dispersed in the polybenzoxazine matrix, attributed to the very low melt viscosity of the benzoxazine resin used, thus resulting in good flow-ability and wetting of the fillers. In addition, flake liked shaped of fillers encapsulated with the polybenzoxazine matrix, indicating substantial interfacial adhesion between the filler

and the matrix. The result was confirmed by no separation of fillers from the polybenzoxazine matrix on fracture surface [36, 62]. Furthermore, the fillers in the composites with high loading were in good contact with each other to give a well-developed electrical pathways and relatively high electrical conductivity useful for bipolar plate utilization.



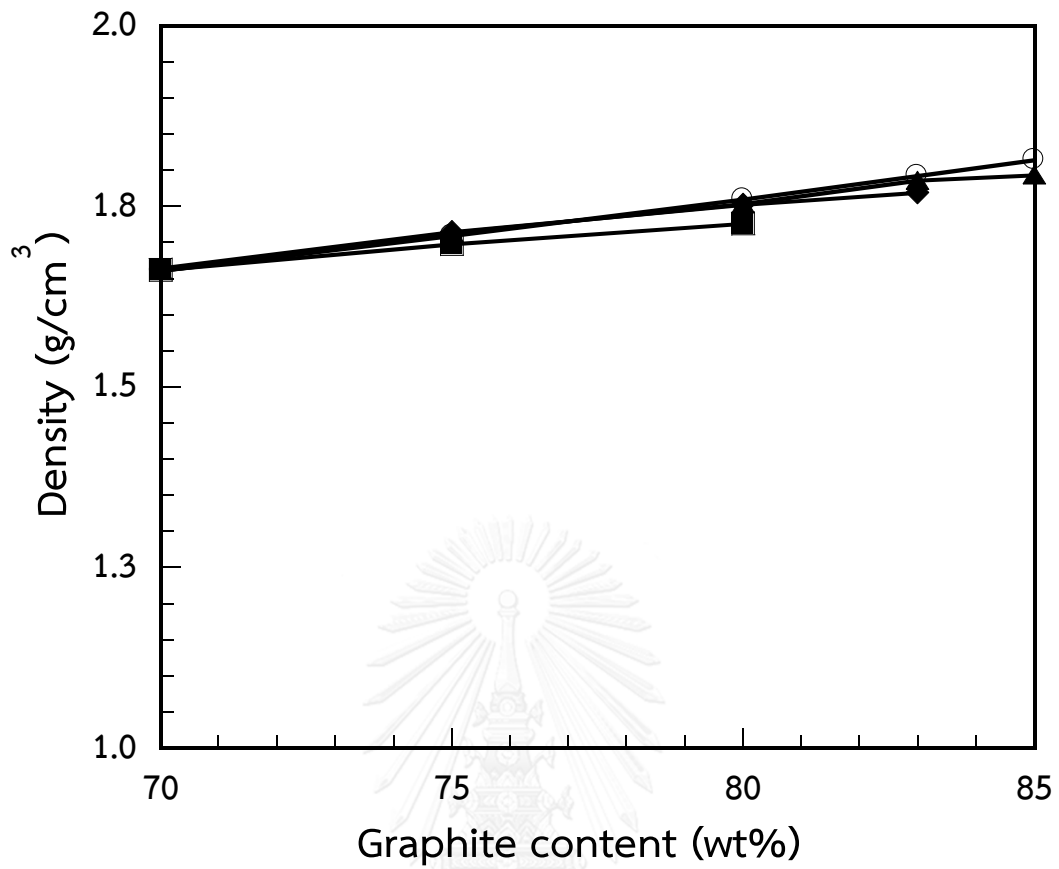


Figure 5.1 Theoretical and actual densities of graphite filled polybenzoxazine composites at different sizes of graphite: (○) theoretical density, (■) <math><50\ \mu\text{m}</math>, (●) $140\ \mu\text{m}$, (▲) $240\ \mu\text{m}$

Table 5.1 The effect of particle size on composite packing densities

Average particle size (μm)	Type	Maximum loading (wt%)
<50	Aggregate	75
140	Aggregate	80
240	Aggregate	83



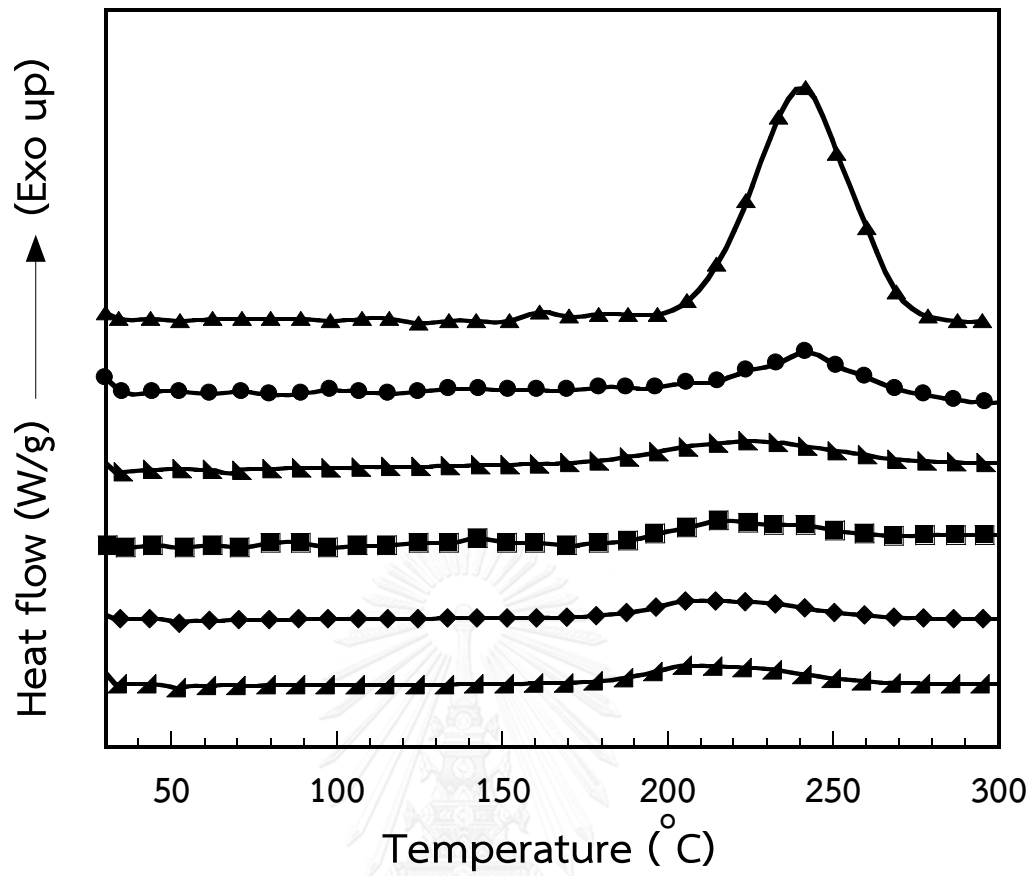


Figure 5.2 DSC thermograms of graphite/graphene filled benzoxazine molding compound at different graphene contents: (▲) neat polybenzoxazine, (●) 83/0wt%, (▴) 80.5/2.5wt%, (■) 78/5wt%, (◆) 75.5/7.5wt%, (▾) 73/10wt%

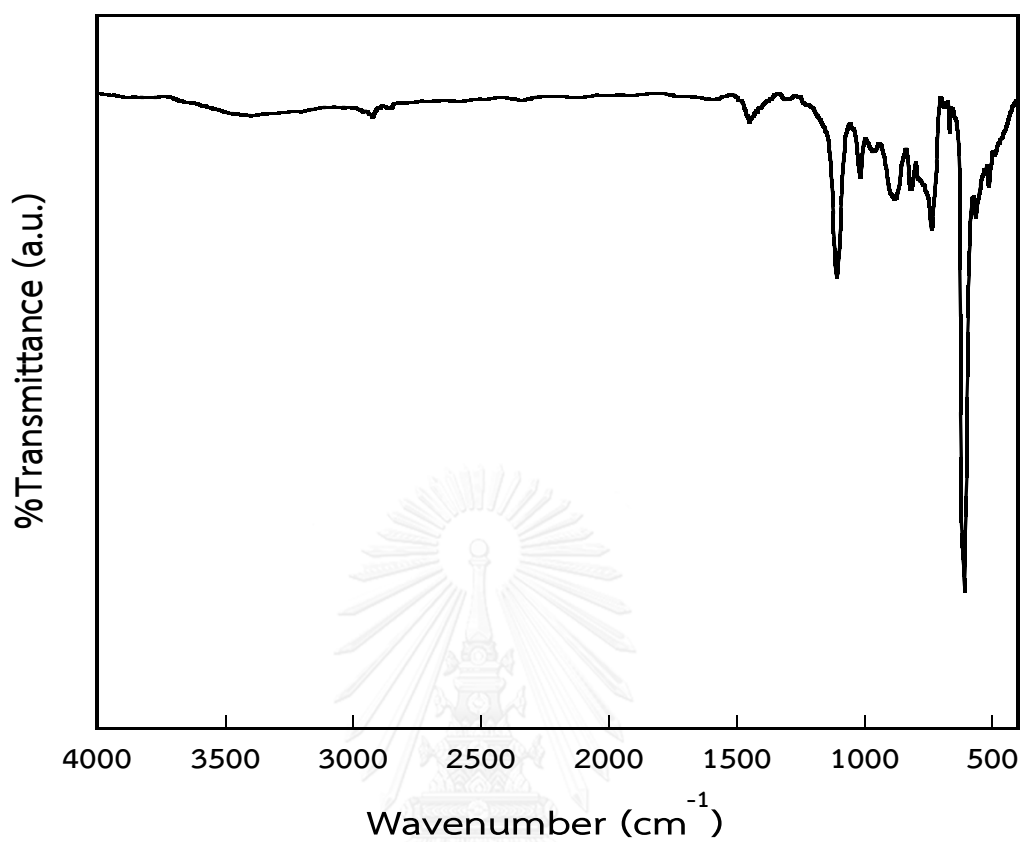


Figure 5.3 FTIR spectra of as-received graphite grad IG-70 from Toyo tanso, Thailand use in this research.

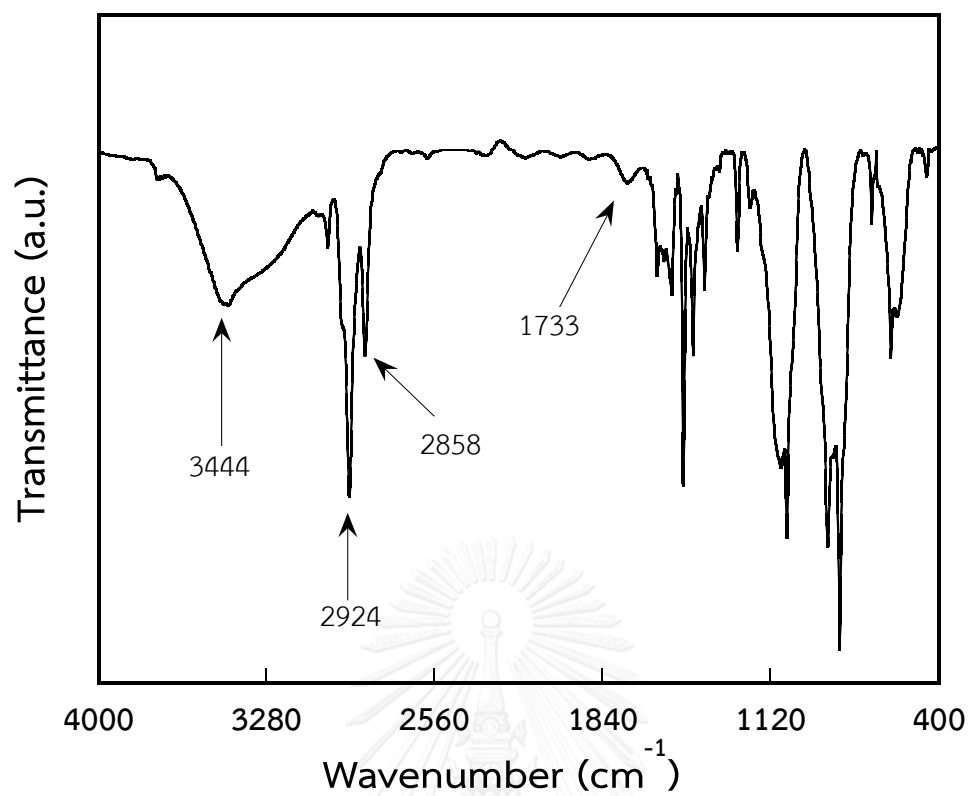


Figure 5.4 FTIR spectra of as-received graphene-grade H from XG Sciences, USA use in this research.

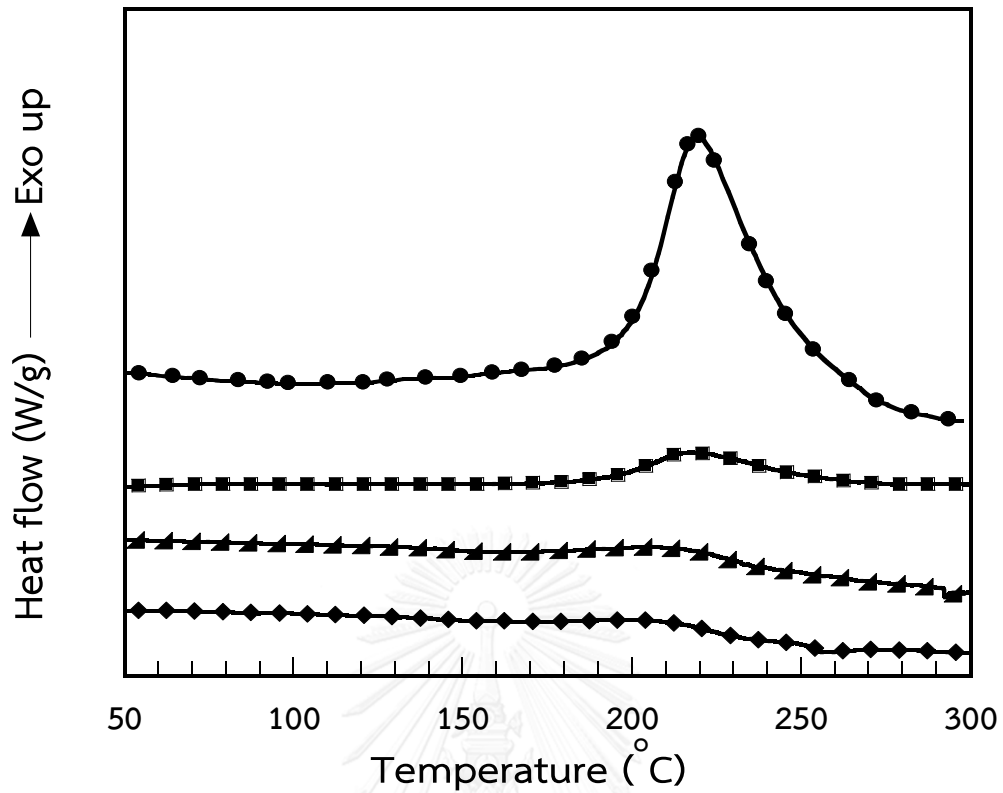


Figure 5.5 DSC thermograms of the composite at 2.5wt% of graphene content with various curing times at 200°C, (●) uncured molding compound, (■) 1 hour, (▲) 2 hours, (◆) 3 hours.

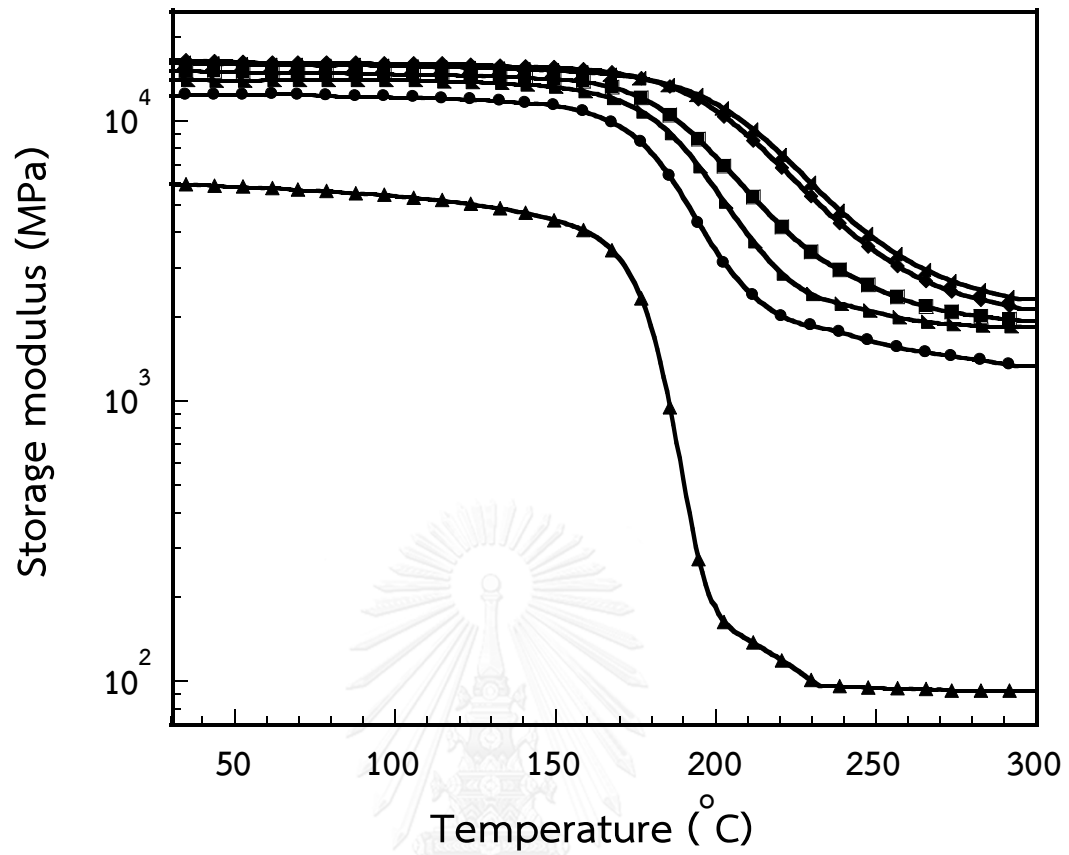


Figure 5.6 DMA thermograms of graphite/graphene filled benzoxazine molding compound at different graphene contents: (▲) neat polybenzoxazine, (●) 83/0wt%, (▴) 80.5/2.5wt%, (■) 78/5wt%, (◆) 75.5/7.5wt%, (▾) 73/10wt%

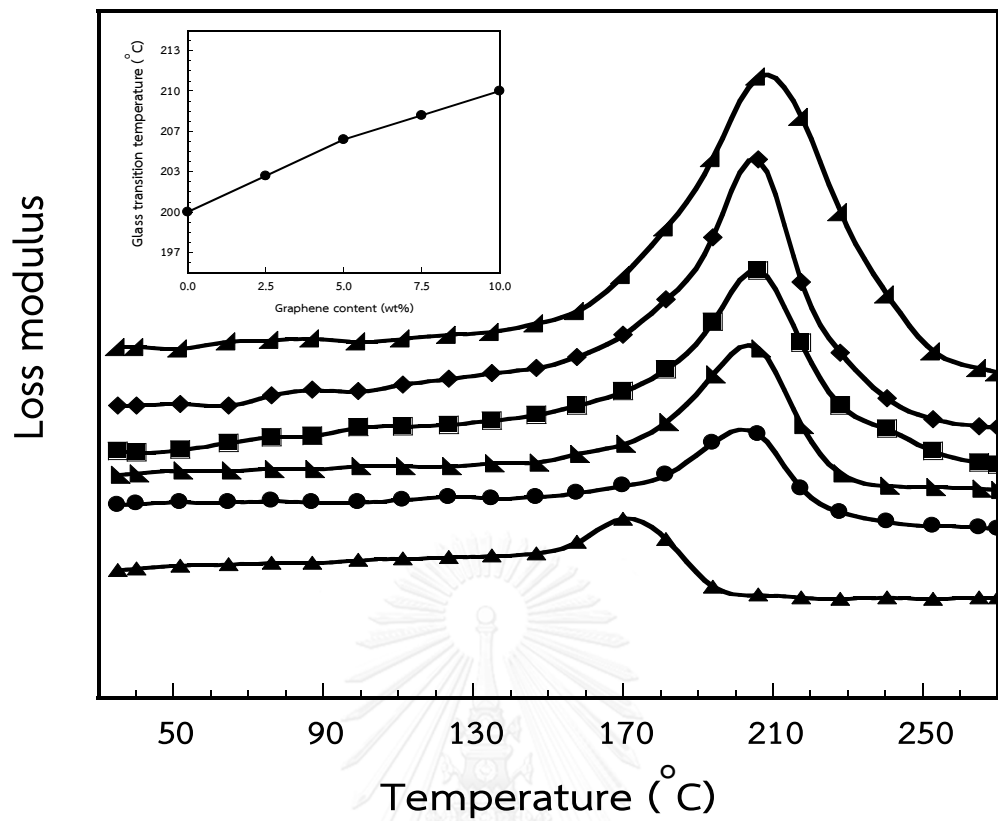


Figure 5.7 DMA thermograms of graphite/graphene filled benzoxazine molding compound at different graphene contents: (▲) neat polybenzoxazine, (●) 83/0wt%, (▴) 80.5/2.5wt%, (■) 78/5wt%, (◆) 75.5/7.5wt%, (▾) 73/10wt%

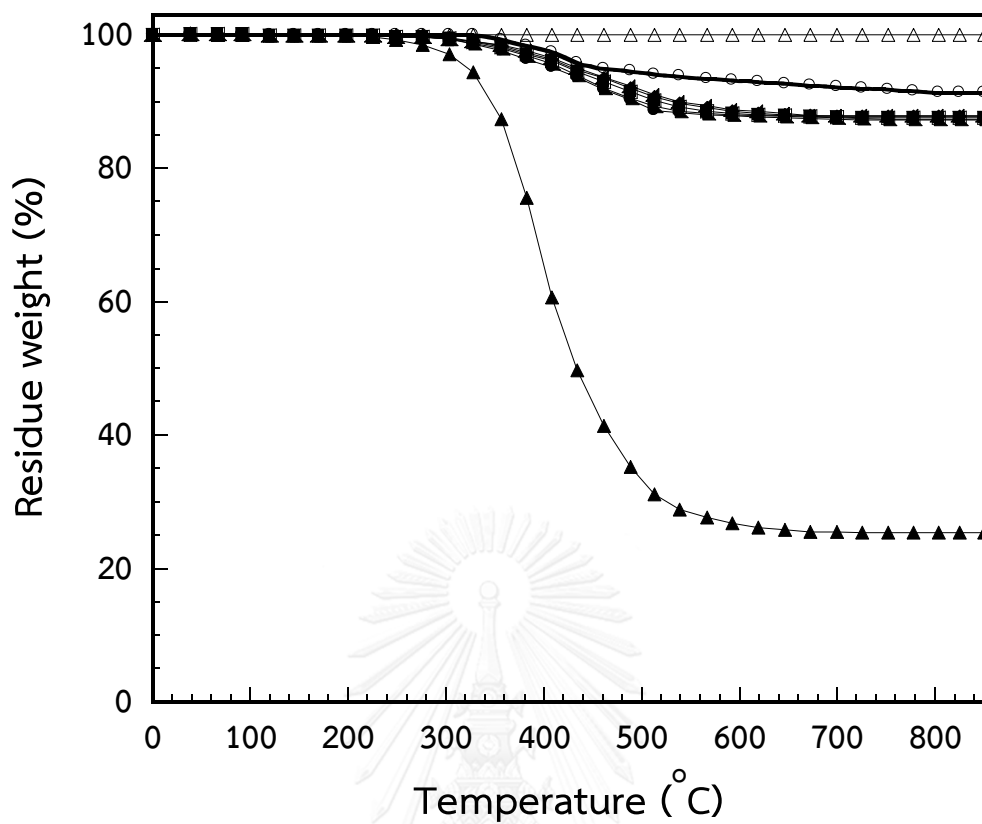


Figure 5.8 TGA thermograms of graphite/graphene filled benzoxazine molding compound at different graphene contents: (▲) neat polybenzoxazine, (●) 83/0wt%, (◄) 80.5/2.5wt%, (■) 78/5wt%, (◆) 75.5/7.5wt%, (►) 73/10wt%, (△) neat graphite, (○) neat graphene

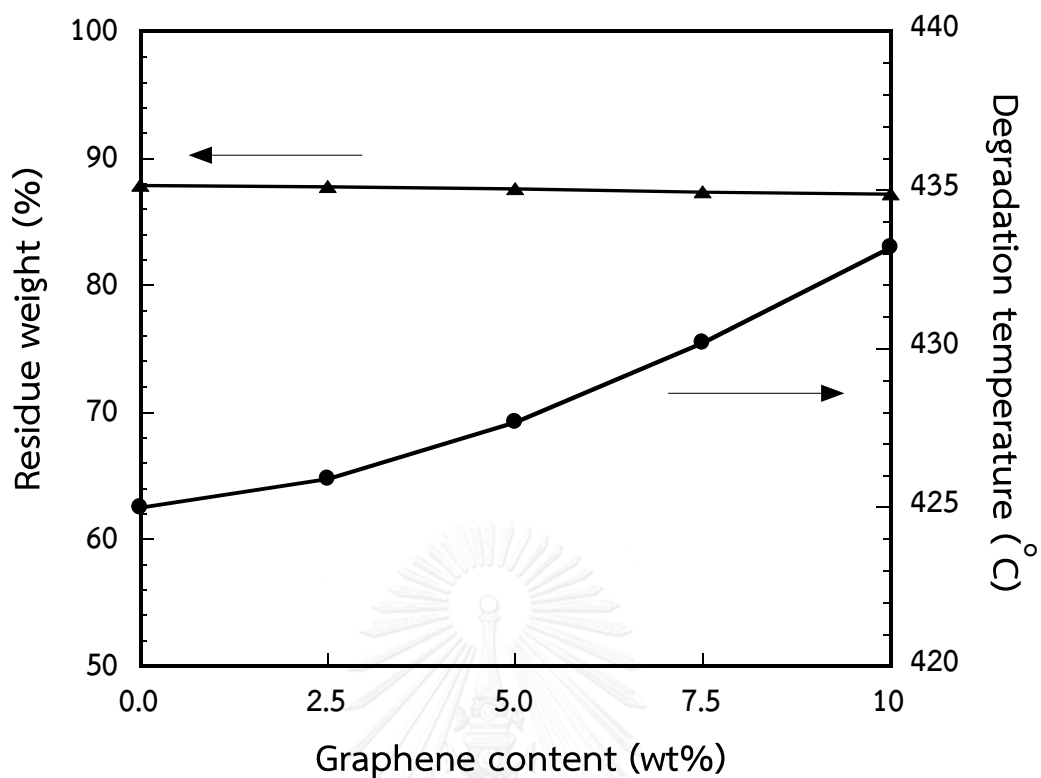


Figure 5.9 Degradation temperature at 5% weight loss and char yield at 800°C of graphite/graphene filled benzoxazine molding compound at different graphene contents: (●) degradation temperature, (▲) char yield

Table 5.2 Thermal characteristics of polybenzoxazine and graphite/graphene filled polybenzoxazine composites.

Graphite content (wt%)	Graphene content (wt%)	T_d ($^{\circ}\text{C}$) at 5% weight loss	Char yield (%) at 800 $^{\circ}\text{C}$ (Experimental)
0	0	320	25.2
83	0	425	87.9
80.5	2.5	425.9	87.8
78.0	5.0	427.7	87.6
75.5	7.5	430.2	87.4
73.0	10.0	433.2	87.2

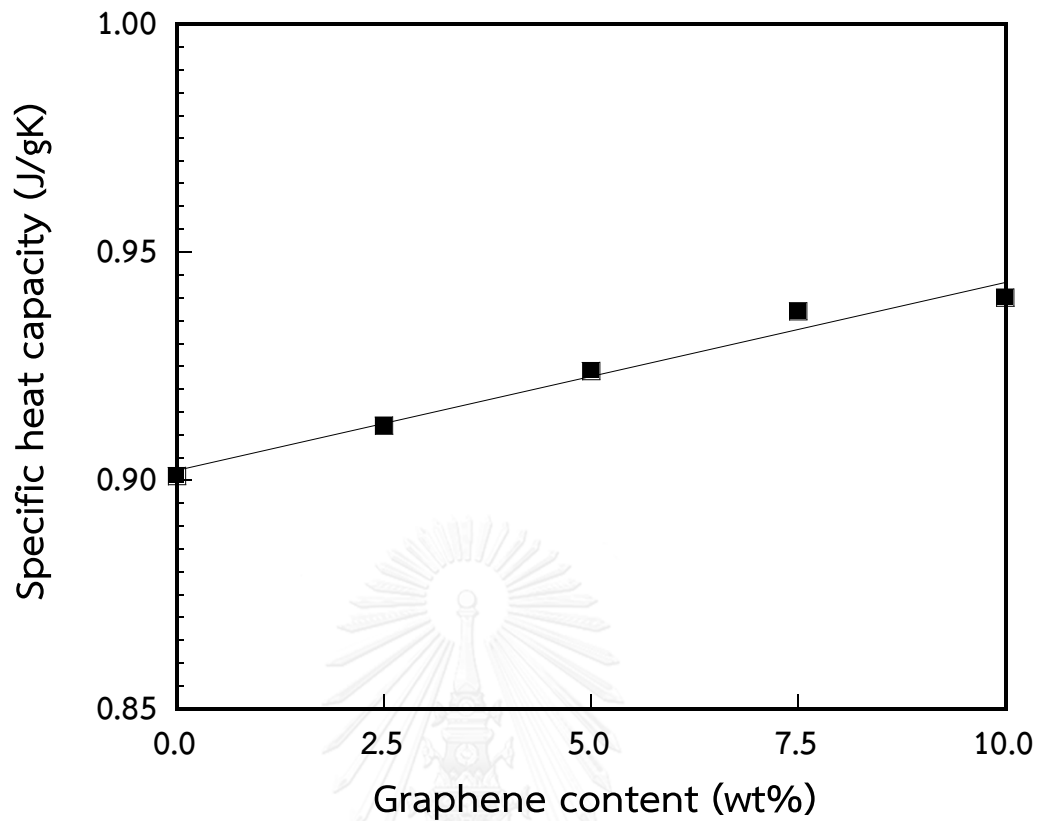


Figure 5.10 Specific heat capacity extrapolated at 25°C of graphite/graphene filled polybenzoxazine as a function of graphene contents.

Table 5.3 Specific heat capacity values of graphite/graphene filled polybenzoxazine at different graphene contents.

Graphite content (wt%)	Graphene content (wt%)	Specific heat capacity ($\text{Jg}^{-1}\text{K}^{-1}$)		Error (%)
		Experimental	Calculated	
0.0	0.0	1.756	-	-
83.0	0.0	0.901	0.938	-0.140
80.5	2.5	0.912	0.944	-0.123
78.0	5.0	0.924	0.950	-0.104
75.5	7.5	0.937	0.957	-0.084
73.0	10.0	0.940	0.963	-0.084

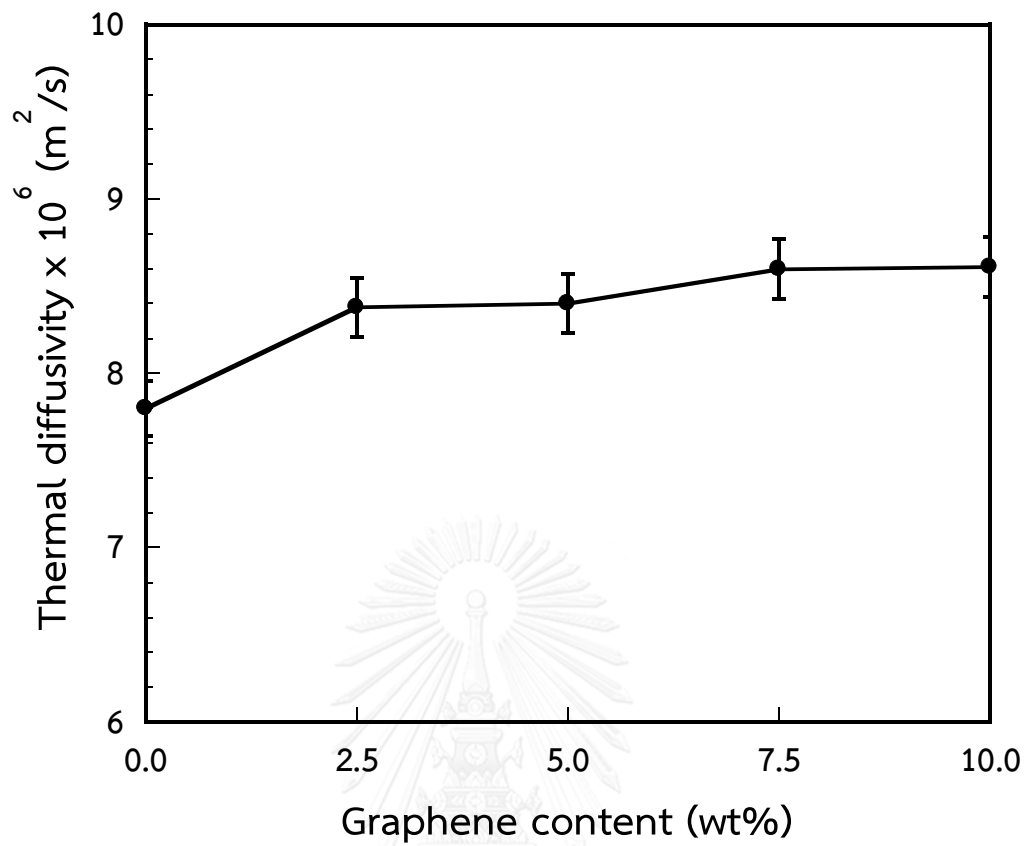


Figure 5.11 Thermal diffusivity at 25°C of graphite/graphene filled polybenzoxazine as a function of graphene contents.

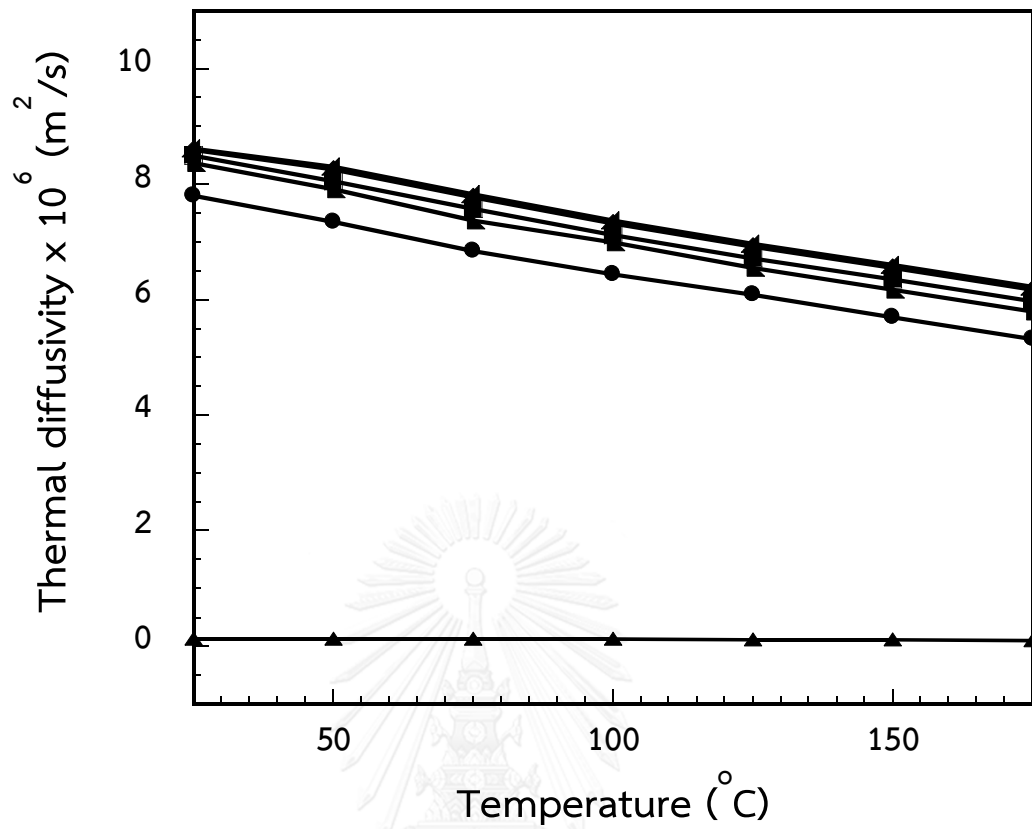


Figure 5.12 Thermal diffusivity of graphite/graphene filled polybenzoxazine composites: (▲) neat polybenzoxazine, (●) 83/0wt%, (▴) 80.5/2.5wt%, (■) 78/5wt%, (◆) 75.5/7.5wt%, (▾) 73/10wt%

Table 5.4 Thermal conductivity of graphite/graphene filled polybenzoxazine composites at 25^oC.

Graphite content (wt%)	Graphene content (wt%)	$\alpha \times 10^6$ (m ² /s)	C _p (J/g K)	ρ (g/cm ³)	k (W/mK)
0.0	0.0	0.13	1.464	1.185	0.23
83.0	0.0	7.80	0.901	1.796	12.6
80.5	2.5	8.38	0.912	1.797	13.7
78.0	5.0	8.40	0.924	1.803	13.9
75.5	7.5	8.60	0.937	1.801	14.5
73.0	10.0	8.61	0.940	1.789	14.4

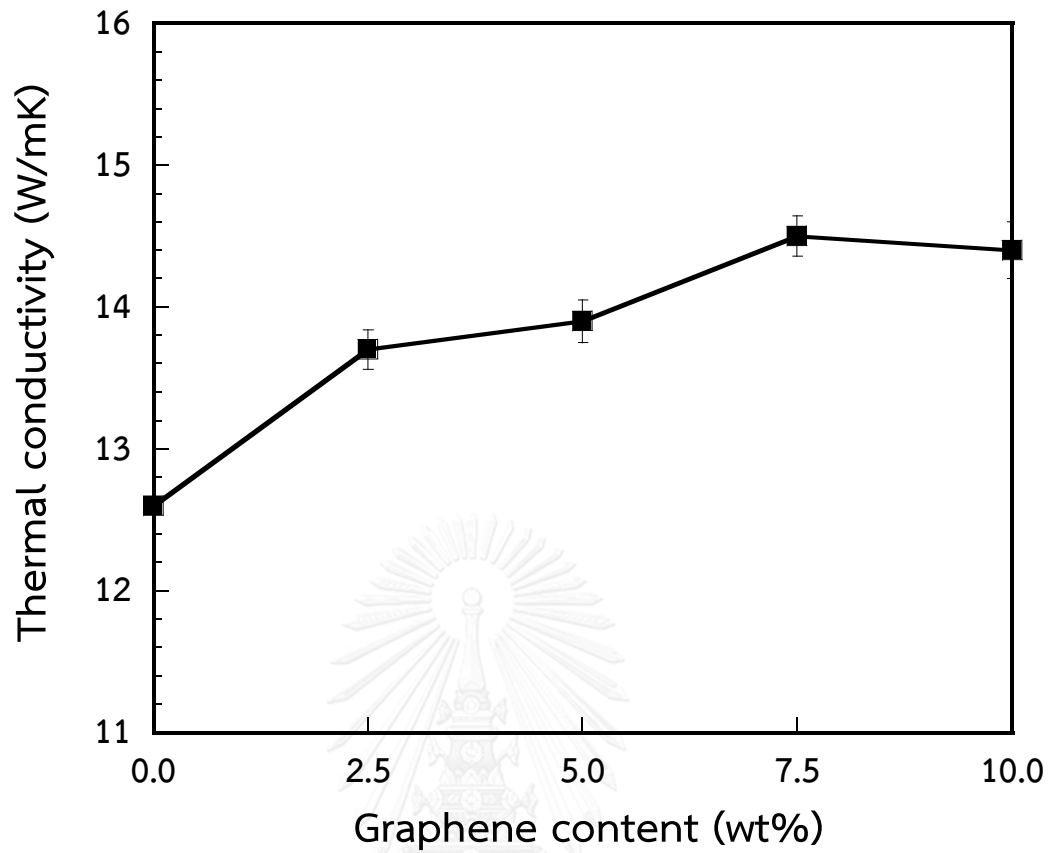


Figure 5.13 Thermal conductivity at 25°C of graphite/graphene filled polybenzoxazine composites as a function of graphene contents.

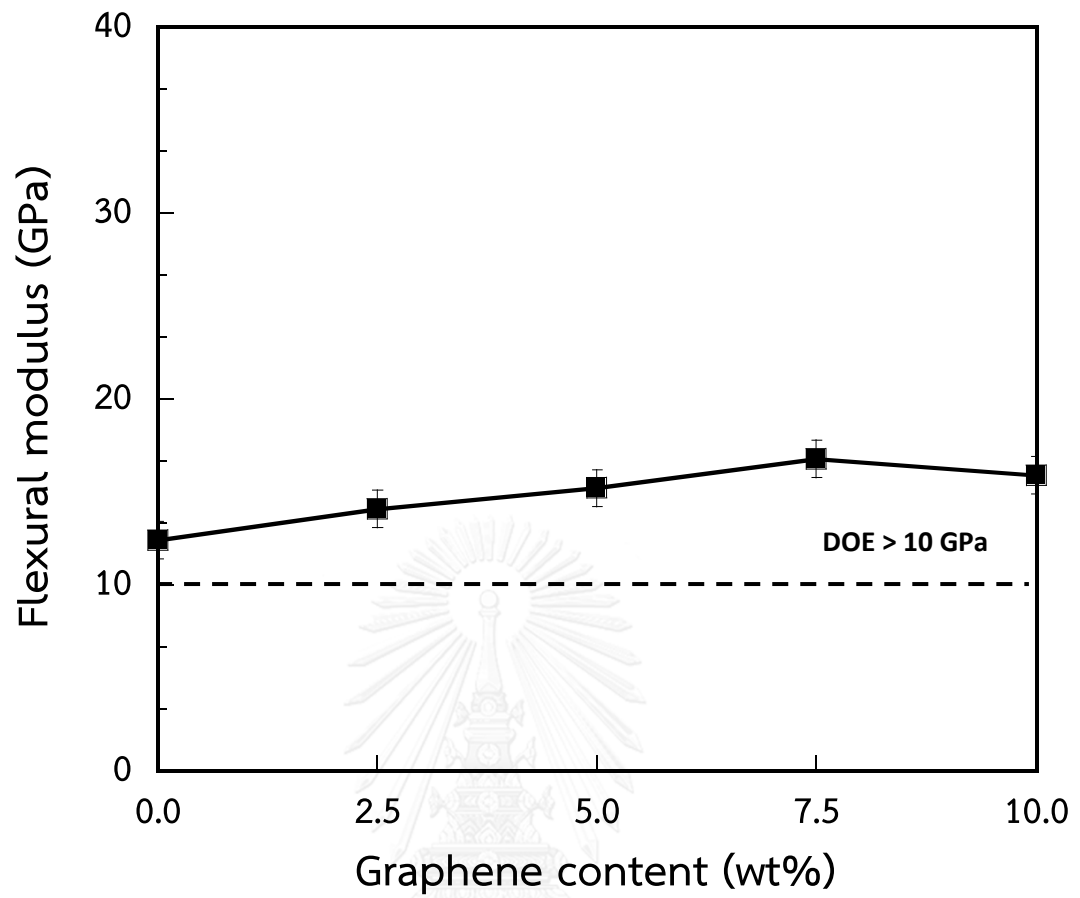


Figure 5.14 Relation between graphene contents and the flexural modulus of graphite/graphene filled polybenzoxazine composites.

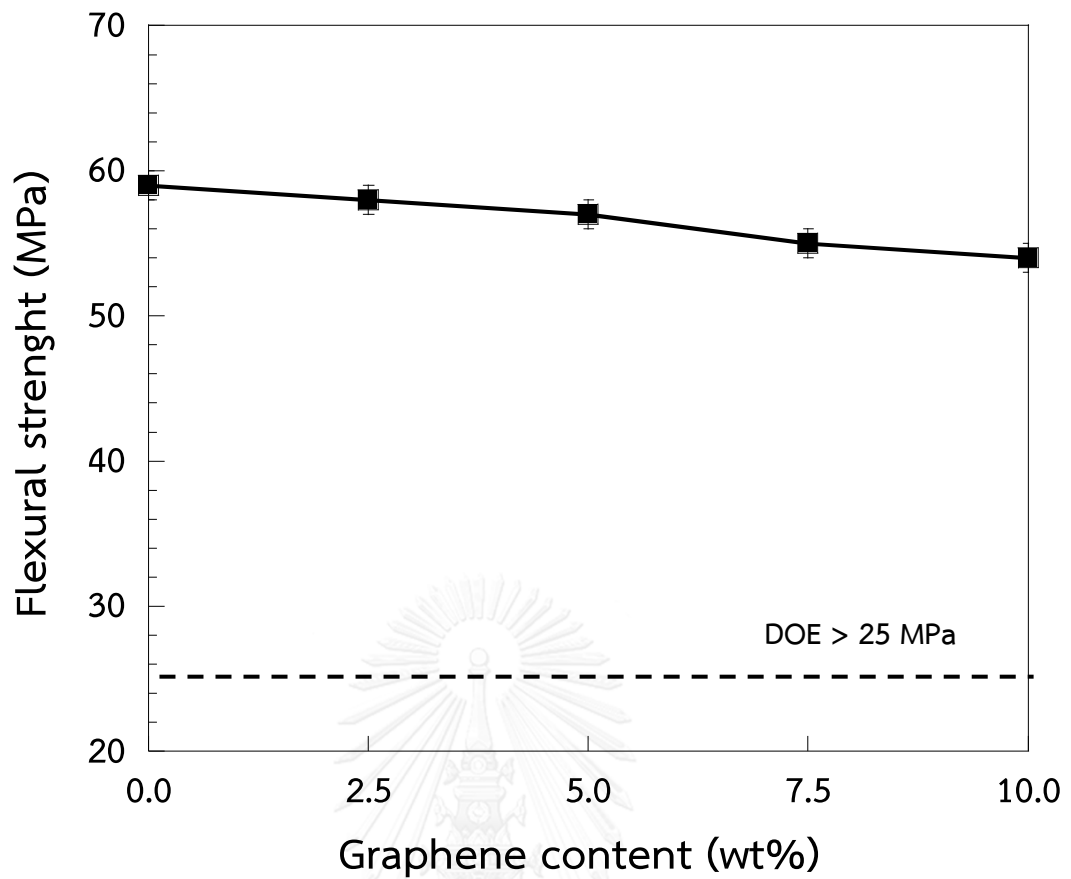


Figure 5.15 Relation between graphene contents and the flexural strength of graphite/graphene filled polybenzoxazine composites.

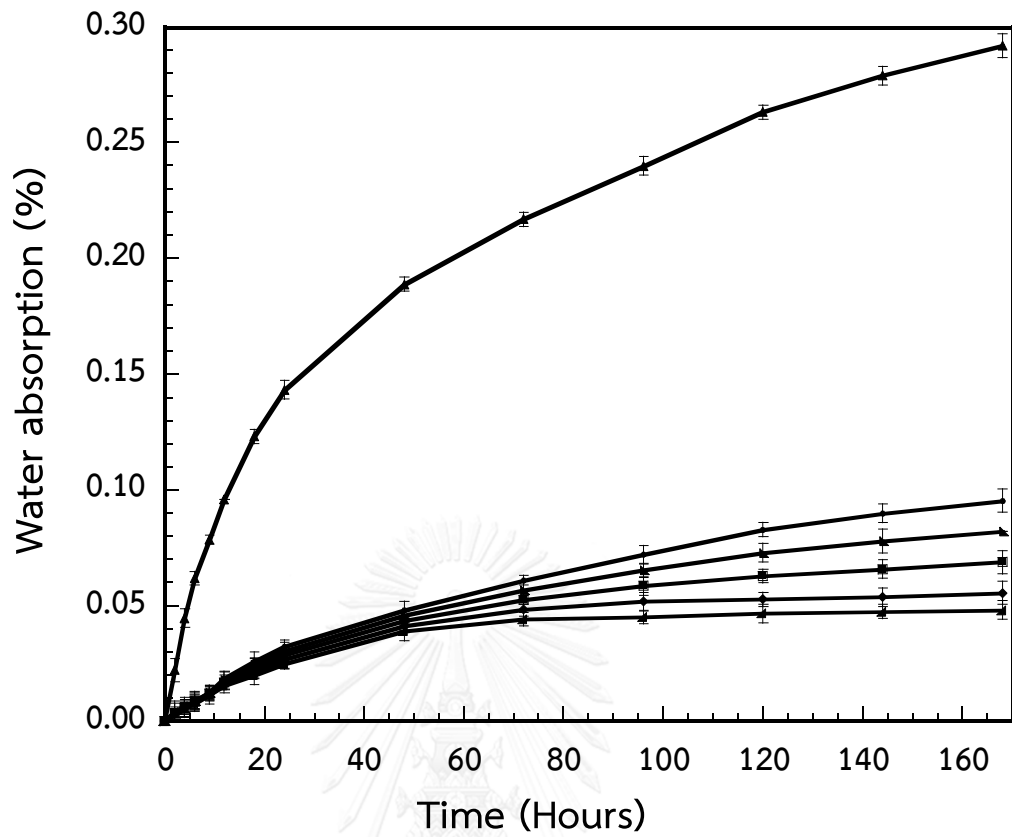


Figure 5.16 Water absorption of graphite/graphene filled polybenzoxazine composites: (▲) neat polybenzoxazine, (●) 83/0wt%, (▲) 80.5/2.5wt%, (■) 78/5wt%, (◆) 75.5/7.5wt%, (▲) 73/10wt%

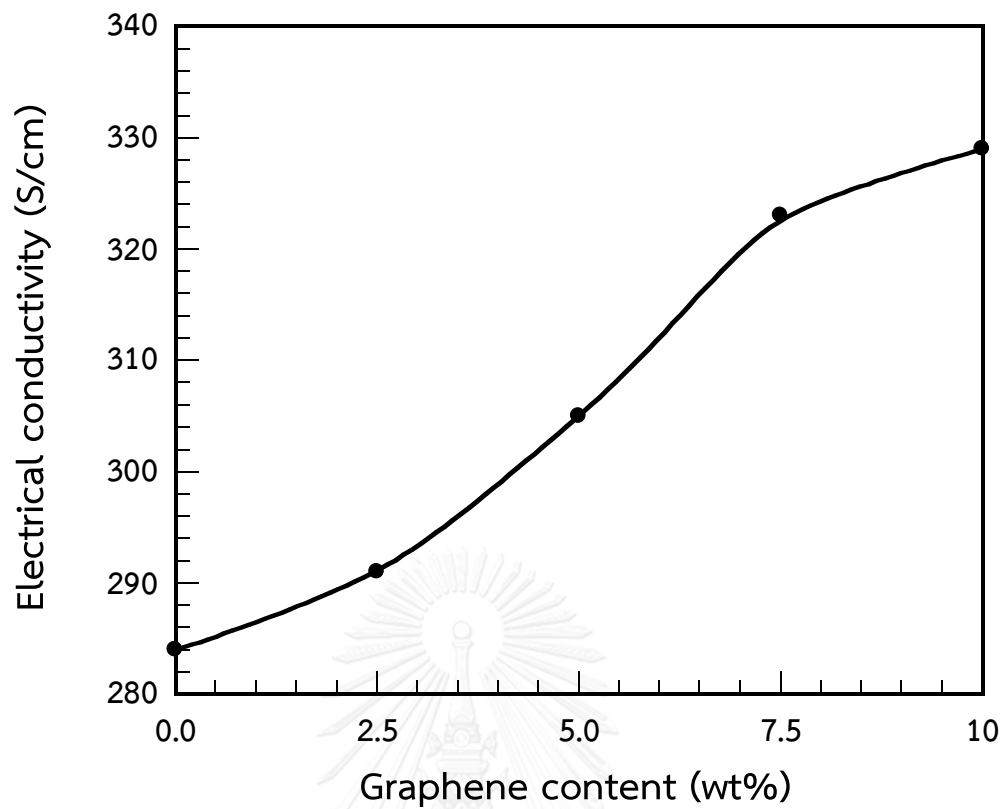
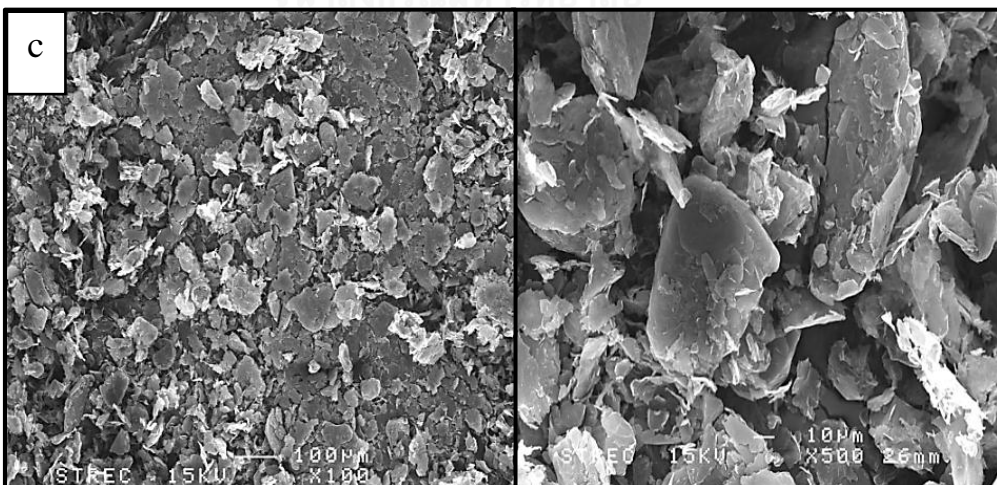
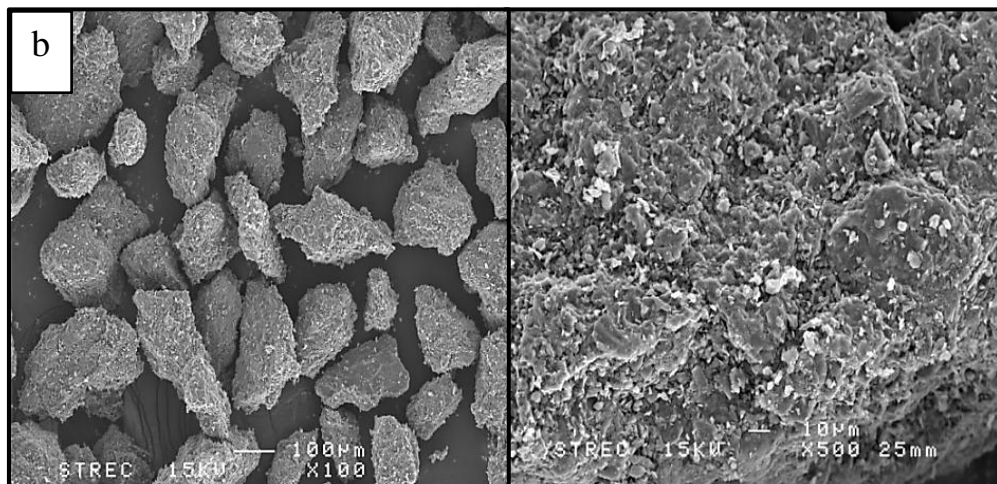
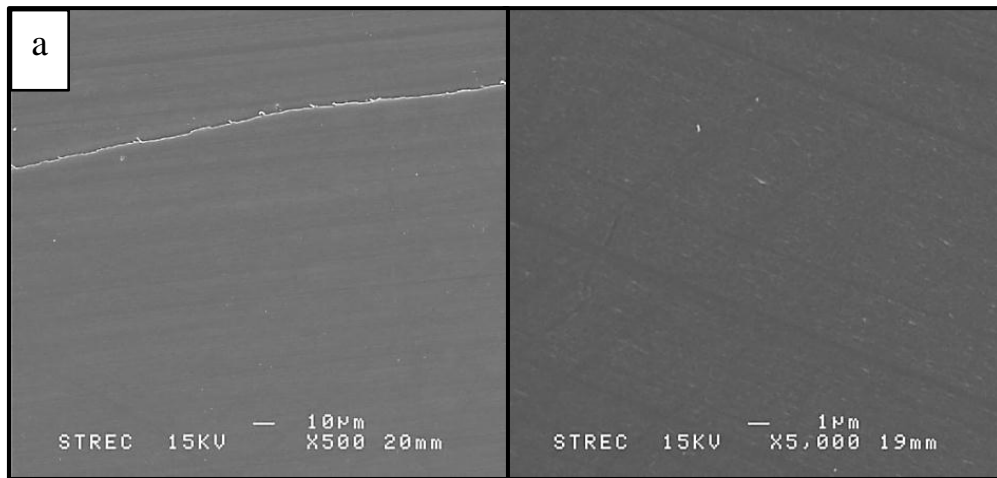


Figure 5.17 Effect of the graphene contents on electrical conductivity (in-plane) of graphite/graphene filled polybenzoxazine composites.



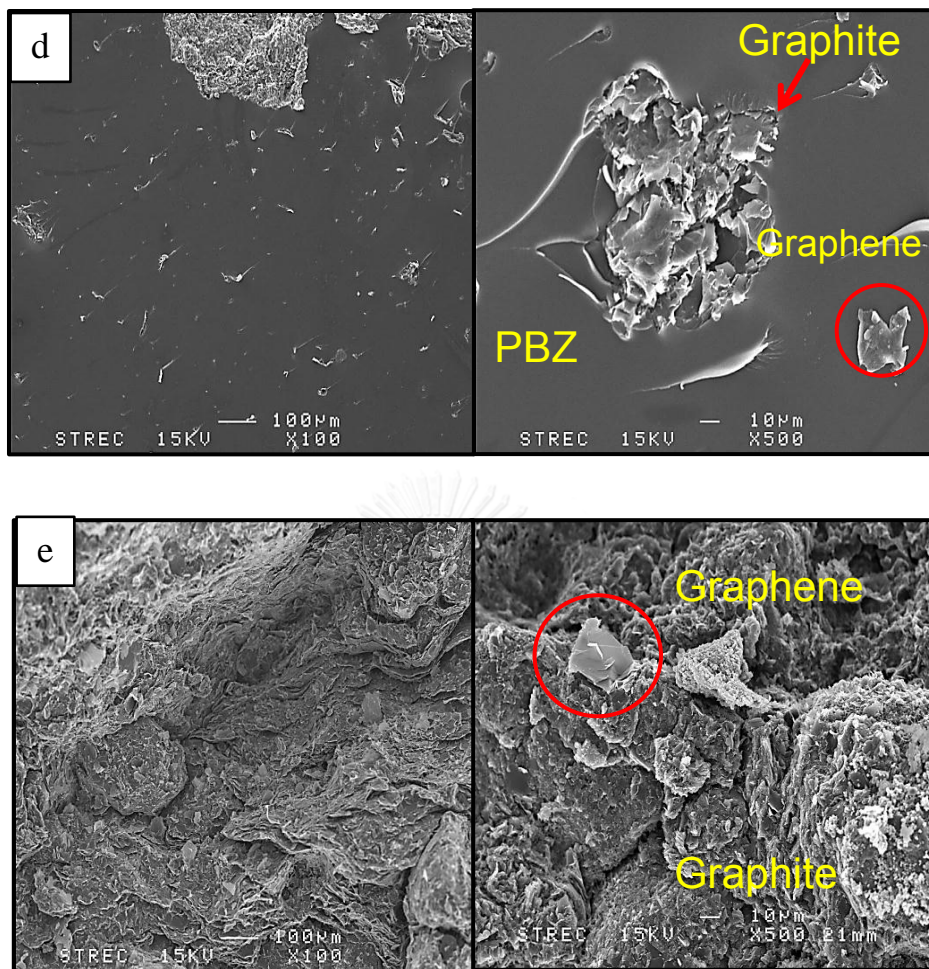


Figure 5.18 SEM micrographs of fracture surface of graphite/graphene filled polybenzoxazine composites:

- (a) neat polybenzoxazine (PBZ)
- (b) pure graphite
- (c) pure graphene
- (d) 0.5/0.5wt% graphite/graphene-filled PBZ
- (e) 80.5/2.5wt% graphite/graphene-filled PBZ

CHAPTER VI

CONCLUSIONS

Highly filled systems of graphite/graphene filled polybenzoxazine with the maximum carbon filler content of 83wt% were achieved in this work. The overall carbon filler content was fixed at 83wt% and varying composition of graphene from 0-10wt% at an expense of the graphite. The composites exhibit various properties highly suitable for a bipolar plate application comparing with most existing system and pass those requirements by the United States Department of Energy (DOE).

Maximum packing density of graphite at sizes 240 μm filled in polybenzoxazine composite exhibits higher the maximum packing density of the composite compared with smaller sizes, which is in good agreement with the theory of particle packing. The actual densities of the composites were measured to be close to the theoretical one suggesting negligible amount of void was presented in the composites.

The DSC experiment revealed that the optimal curing condition to obtain the fully-cured specimens of the graphite/graphene filled polybenzoxazine composites was by heating at 200°C for 3 hours in a hydraulic hot-pressed machine at 15 MPa. The mechanical and thermal properties of graphite/graphene filled polybenzoxazine composites at different graphene loadings in the range 0 to 10wt% tended to

increase with increasing graphene loadings. The glass transition temperature of graphite/graphene filled polybenzoxazine composites were found to increase with increasing graphene contents, due to the substantial bonding between the polymer and the filler. The degradation temperatures (at 5% weight loss under nitrogen atmosphere) and solid residue (at 800°C) of the composites were also observed to substantially increase with increasing the graphene contents.

Moreover, modulus of the graphite/graphene filled polybenzoxazine composites was significantly improved by the presence of the graphene even at only few percent of the filler. The storage modulus of the composite also exhibited the similar trend with the flexural modulus whereas the flexural strength of the composite decreased with an increasing graphene content due to the presence of interface between the filler and the matrix of these heterogeneous systems. Furthermore, water absorption of graphite/graphene filled polybenzoxazine composites was significantly suppressed by the increasing of the graphene contents.

Scanning electron micrographs exhibits good interfacial adhesion with tight interfaces between filler and the polybenzoxazine matrix. The polybenzoxazine matrix can wetting high filler loading.

Finally, thermal conductivity and electrical conductivity of graphite/graphene filled polybenzoxazine composites were observed found to increase with increasing the graphene contents in a non-linear manner. Due to the fact that, large size of

graphite, should be beneficial in producing a small number of interfaces and adding a small amount of graphene nanofillers should enhance the interaction between the graphite due to the presence of nanofillers between them. The filler can form continuous conductive path.

The obtained mechanical properties and electrical conductivity of the highly filled graphite/graphene filled polybenzoxazine composites are found to be highly attractive for bipolar plates in polymer electrolyte membrane fuel cells (PEMFCs) application. Those properties were found to exceed those requirements set by DOE.



REFERENCES

- [1] Boyaci San, F.G., Isik-Gulsac , I., and Osman, O., Analysis of the polymer composite bipolar plate properties on the performance of PEMFC (polymer electrolyte membrane fuel cells) by RSM (response surface methodology). Energy, 2013. 55: p. 1067-1075.
- [2] Kang, S.-J., Kim, D.O., Lee, J.-H., Lee, P.-C., Lee, M.-H., Lee, Y., Lee, J.Y., Choi, H.R., Lee, J.-H., Oh, Y.-S., and Nam, J.-D., Solvent-assisted graphite loading for highly conductive phenolic resin bipolar plates for proton exchange membrane fuel cells. Journal of Power Sources, 2010. 195(12): p. 3794-3801.
- [3] Fu, Y., Lin, G., Hou, M., Wu, B., Shao, Z., and Yi, B., Carbon-based films coated 316L stainless steel as bipolar plate for proton exchange membrane fuel cells. International Journal of Hydrogen Energy, 2009. 34(1): p. 405-409.
- [4] *Technical plane fuel cells*. 2015; Available from: http://www1.eere.energy.gov/hydrogenandfuelcells/mypp/pdfs/fuel_cells.pdf.
- [5] Taherian, R., A review of composite and metallic bipolar plates in proton exchange membrane fuel cell: Materials, fabrication, and material selection. Journal of Power Sources, 2014. 265: p. 370-390.
- [6] Kim, M., Lim, J.W., Kim, K.H., and Lee, D.G., Bipolar plates made of carbon fabric/phenolic composite reinforced with carbon black for PEMFC. Composite Structures, 2013. 96: p. 569-575.
- [7] Kim, J.W., Kim, N.H., Kuilla, T., Kim, T.J., Rhee, K.Y., and Lee, J.H., Synergy effects of hybrid carbon system on properties of composite bipolar plates for fuel cells. Journal of Power Sources, 2010. 195(17): p. 5474-5480.
- [8] Ishida, H. and Rimdusit, S., Very high thermal conductivity obtained by boron nitride-filled polybenzoxazine. Thermochimica Acta, 1998. 320(1-2): p. 177-186.
- [9] Kim, H., Abdala, A.A., and Macosko, C.W., Graphene/Polymer Nanocomposites. Macromolecules, 2010. 43(16): p. 6515-6530.

- [10] Rimdusit S., Jubsilp C., and Tipipakorn S., Alloys and Composites of Polybenzoxazines. 2013, Singapore: Springer.
- [11] Greenwood, P.S. Polymeric bipolar plates for PEM fuel cells: experimental and modeling approach to assess factors influencing performance. Loughborough University, 2010.
- [12] López Gaxiola, D., Characterization Of Thermal And Mechanical Properties Of Polypropylene-Based Composites For Fuel Cell Bipolar Plates And Development Of Educational Tools In Hydrogen And Fuel Cell Technologies, ed. M.T. University. 2011: Dissertation.
- [13] Wang, Y., Chen, K.S., Mishler, J., Cho, S.C., and Adroher, X.C., A review of polymer electrolyte membrane fuel cells: Technology, applications, and needs on fundamental research. Applied Energy, 2011. 88(4): p. 981-1007.
- [14] Bipolar plates. 2015; Available from: <http://www.bac2.co.uk/bipolar-plates>.
- [15] Kim, M., Yu, H.N., Lim, J.W., and Lee, D.G., Bipolar plates made of plain weave carbon/epoxy composite for proton exchange membrane fuel cell. International Journal of Hydrogen Energy, 2012. 37(5): p. 4300-4308.
- [16] Włodarczyk, R., Dudek, A., Kobylecki, R., and Bis, Z., Corrosion Resistance. Properties of Graphite Sinters for Bipolar Plates in Fuel Cells. 2012.
- [17] Hermann, A., Chaudhuri, T., and Spagnol, P., Bipolar plates for PEM fuel cells: A review. International Journal of Hydrogen Energy, 2005. 30(12): p. 1297-1302.
- [18] Dhakate, S.R., Mathur, R.B., Kakati, B.K., and Dhami, T.L., Properties of graphite-composite bipolar plate prepared by compression molding technique for PEM fuel cell. International Journal of Hydrogen Energy, 2007. 32(17): p. 4537-4543.
- [19] Mehta, V. and Cooper, J.S., Review and analysis of PEM fuel cell design and manufacturing. Journal of Power Sources, 2003. 114(1): p. 32-53.
- [20] Cooper, J.S., Design analysis of PEMFC bipolar plates considering stack manufacturing and environment impact. Journal of Power Sources, 2004. 129(2): p. 152-169.

- [21] Maheshwari, P.H., Mathur, R.B., and Dhama, T.L., Fabrication of high strength and a low weight composite bipolar plate for fuel cell applications. Journal of Power Sources, 2007. 173(1): p. 394-403.
- [22] Tawfik, H., Hung, Y., and Mahajan, D., Metal bipolar plates for PEM fuel cell— A review. Journal of Power Sources, 2007. 163(2): p. 755-767.
- [23] Antunes, R.A., de Oliveira, M.C.L., Ett, G., and Ett, V., Carbon materials in composite bipolar plates for polymer electrolyte membrane fuel cells: A review of the main challenges to improve electrical performance. Journal of Power Sources, 2011. 196(6): p. 2945-2961.
- [24] Yeetsorn R., Fowler M. W., and Tzoganakis C., Chapter 16 Nanocomposites with Unique Properties and Applications in Medicine and Industry, 2011.
- [25] Pierson, H.O., 3 - Graphite Structure and Properties, in Handbook of Carbon, Graphite, Diamonds and Fullerenes. 1993, William Andrew Publishing: Oxford. p. 43-69.
- [26] Hehr, B.D. High Temperature Graphite Simulations Using Molecular Dynamics. Graduate Faculty of North Carolina State University, 2007.
- [27] Pyrolytic graphite 2015; Available from: <http://www.kdd1.com/emc/011/emc-sarmal1.html>.
- [28] Ferro-Ceramic Grinding Inc. 2015; Available from: http://www.ferroc ceramic.com/graphite_table.htm.
- [29] Webb, T.C. and Stewart, H.J. Graphite. New Brunswick Department of Natural Resources; Minerals, Policy and Planning Division, Mineral Commodity Profile 3, 2009.
- [30] The graphene story. 2015; Available from: <http://www.graphene.manchester.ac.uk/story/>.
- [31] Graphene. 2015; Available from: <http://www.grapheneleaderscanada.com/what-is-graphene/>.
- [32] Graphene properties. 2015; Available from: <http://www.explainthatstuff.com/graphene.html>.
- [33] Ishida, H., Process of benzoxazine compounds in solventless systems U.S. Patent 5,543,516, 1996.

- [34] Lide, D.R., Handbook of Chemistry and Physics ed. t. edition. 2004, CRC Press, New York.
- [35] Ishida, H. and Sanders, D.P., Improved thermal and mechanical properties of polybenzoxazines based on alkyl-substituted aromatic amines. Journal of Polymer Science Part B: Polymer Physics, 2000. 38: p. 3289-3301.
- [36] Dueramae, I., Pengdam, A., and Rimdusit, S., Highly filled graphite polybenzoxazine composites for an application as bipolar plates in fuel cells. Journal of Applied Polymer Science, 2013. 130(6): p. 3909-3918.
- [37] Plengudomkit, R., Okhawilai, M., and Rimdusit, S., Highly filled graphene-benzoxazine composites as bipolar plates in fuel cell applications. Polymer Composites, 2014: p. n/a-n/a.
- [38] Kakati, B.K., Ghosh, A., and Verma, A., Efficient composite bipolar plate reinforced with carbon fiber and graphene for proton exchange membrane fuel cell. International Journal of Hydrogen Energy, 2013. 38(22): p. 9362-9369.
- [39] Ghosh, A., Goswami, P., Mahanta, P., and Verma, A., Effect of carbon fiber length and graphene on carbon-polymer composite bipolar plate for PEMFC. Journal of Solid State Electrochemistry, 2014. 18(12): p. 3427-3436.
- [40] Huang, K.-J., Niu, D.-J., Sun, J.-Y., Han, C.-H., Wu, Z.-W., Li, Y.-L., and Xiong, X.-Q., Novel electrochemical sensor based on functionalized graphene for simultaneous determination of adenine and guanine in DNA. Colloids and Surfaces B: Biointerfaces, 2011. 82(2): p. 543-549.
- [41] Jiang, X. and Drzal, L.T., Exploring the potential of exfoliated graphene nanoplatelets as the conductive filler in polymeric nanocomposites for bipolar plates. Journal of Power Sources, 2012. 218: p. 297-306.
- [42] Wang, X., Yang, H., Song, L., Hu, Y., Xing, W., and Lu, H., Morphology, mechanical and thermal properties of graphene-reinforced poly(butylene succinate) nanocomposites. Composites Science and Technology, 2011. 72(1): p. 1-6.
- [43] Rimdusit, S., Kampangsaeree, N., Tanthapanichakoon, W., Takeichi, T., and Suppakarn, N., Development of wood-substituted composites from highly

- filled polybenzoxazine–phenolic novolac alloys. Polymer Engineering & Science, 2007. 47(2): p. 140-149.
- [44] XG Sciences the material difference, *Technical data sheet of XGnP® Grade H product characteristics*. 2016 March 14]; Available from: <http://xgsciences.com/>.
- [45] Yadav, S.K. and Cho, J.W., Functionalized graphene nanoplatelets for enhanced mechanical and thermal properties of polyurethane nanocomposites. Applied Surface Science, 2013. 266: p. 360-367.
- [46] Sheshmani, S., Ashori, A., and Arab Fashapoyeh, M., Wood plastic composite using graphene nanoplatelets. International Journal of Biological Macromolecules, 2013. 58: p. 1-6.
- [47] Jubsilp, C., Panyawanitchakun, C., and Rimdusit, S., Flammability and thermomechanical properties of dianhydride-modified polybenzoxazine composites reinforced with carbon fiber. Polymer Composites, 2013. 34(12): p. 2067-2075.
- [48] Ishida, H. and Rimdusit, S., Heat Capacity Measurement of Boron Nitride-filled Polybenzoxazine: The composite structure-insensitive property. Journal of Thermal Analysis and Calorimetry, 1999. 58(3): p. 497-507.
- [49] *Thermal diffusivity*. 2016 June 4]; Available from: https://en.wikipedia.org/wiki/Thermal_diffusivity.
- [50] Xu, Y., Ray, G., and Abdel-Magid, B., Thermal behavior of single-walled carbon nanotube polymer–matrix composites. Composites Part A: Applied Science and Manufacturing, 2006. 37(1): p. 114-121.
- [51] Mahanta, N.K., Loos, M.R., Manas Zloczower, I., and Abramson, A.R., Graphite–graphene hybrid filler system for high thermal conductivity of epoxy composites. Journal of Materials Research, 2015. 30(07): p. 959-966.
- [52] Tian, X., Itkis, M.E., Bekyarova, E.B., and Haddon, R.C., Anisotropic Thermal and Electrical Properties of Thin Thermal Interface Layers of Graphite Nanoplatelet-Based Composites. Scientific reports, 2013.
- [53] Li, B. and Zhong, W.-H., Review on polymer/graphite nanoplatelet nanocomposites. Journal of materials science, 2011. 46(17): p. 5595-5614.

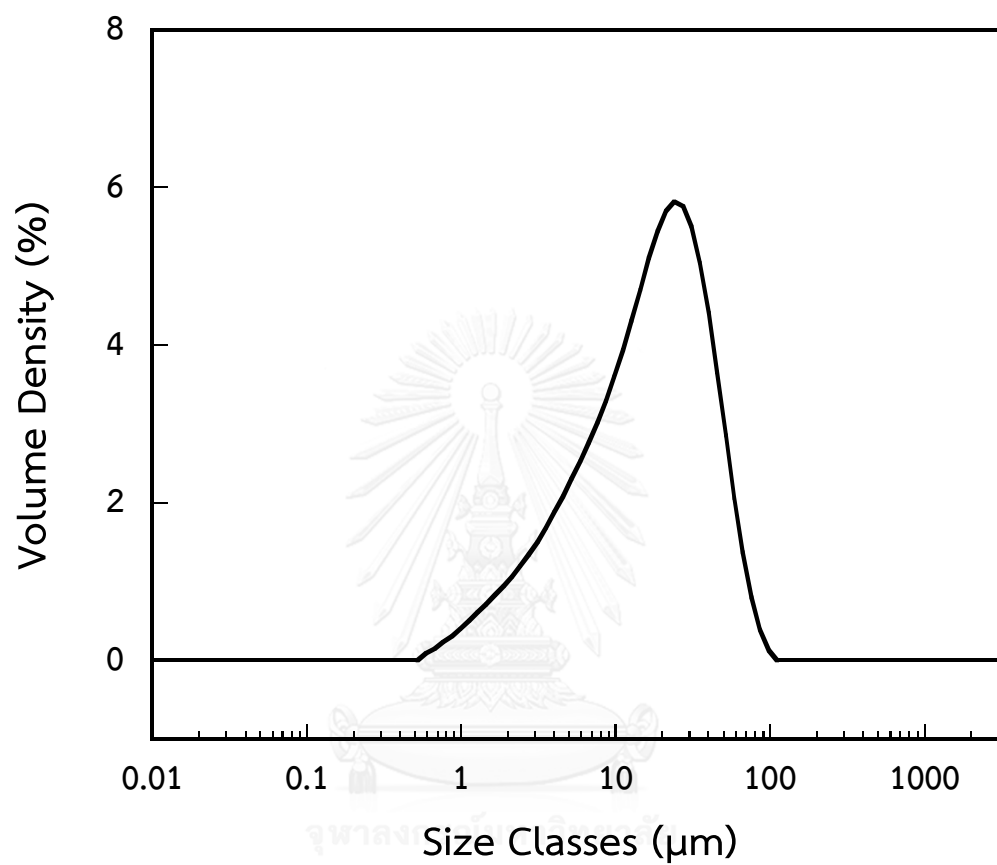


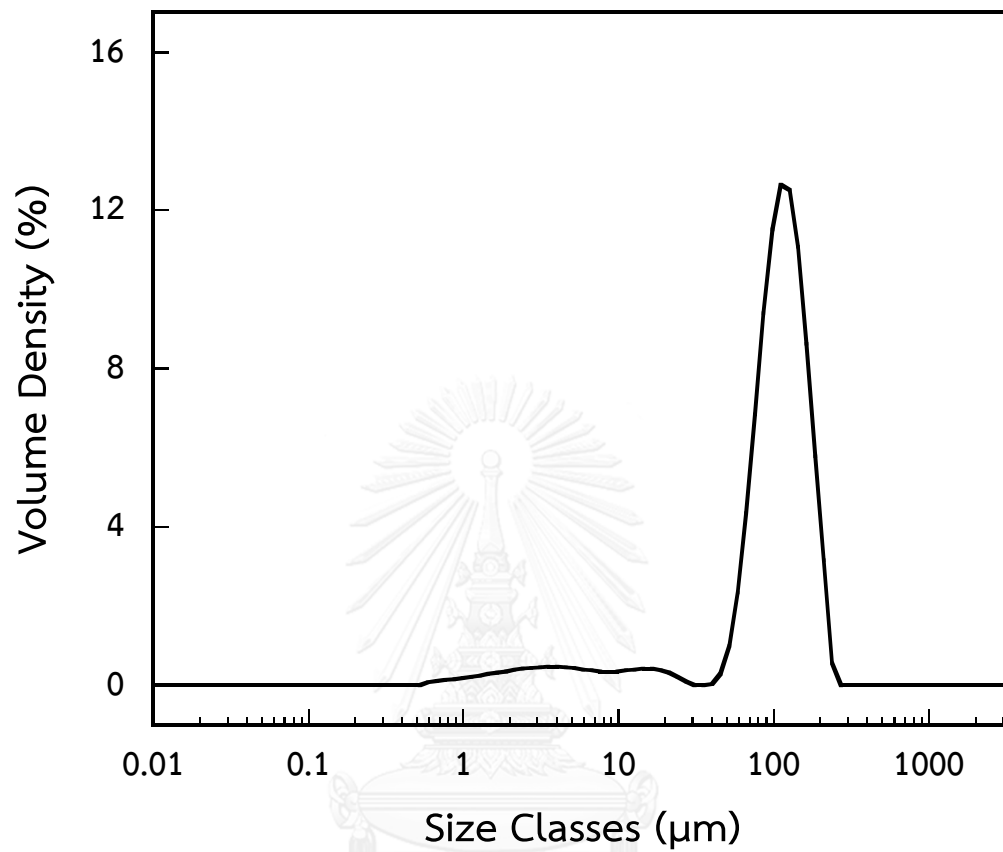
APPENDIX

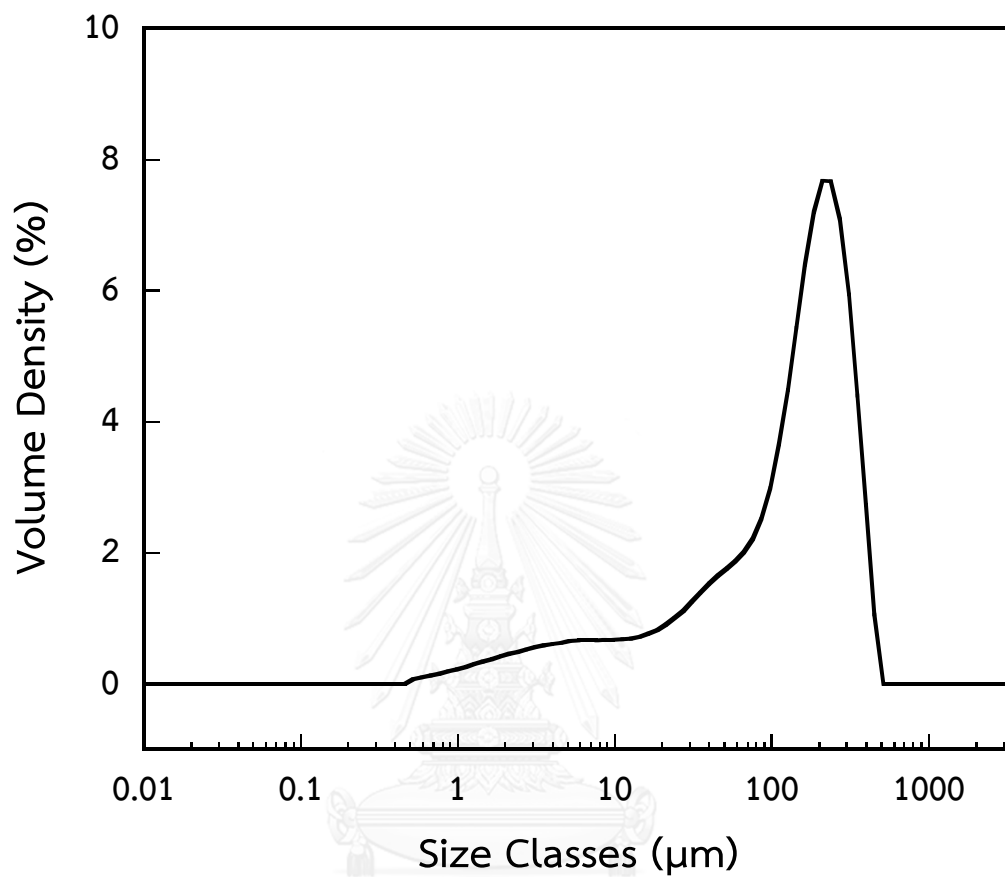
จุฬาลงกรณ์มหาวิทยาลัย
CHULALONGKORN UNIVERSITY

APPENDIX A Average graphite aggregate size

Appendix A-1 Average graphite aggregate size <math>< 50 \mu\text{m}</math>



Appendix A-2 Average graphite aggregate size 140 μm 

Appendix A-3 Average graphite aggregate size 240 μm 

VITA

Ms. Manlika Phuangngamphan was born in Saraburi, Thailand. She graduated at high school level in 2010 from Nongkhae Sorakitpittaya School. She received the Bachelor's Degree of Engineering with a major in Chemical Engineering from the Faculty of Engineer, Thammasat University, Thailand in 2014. After graduation, she entered study for a Master's Degree of Chemical Engineering at the Department of Chemical Engineering, Faculty of Engineering, Chulalongkorn University.



